

3.1 Turbine Combustion Phenomena

TURBINE COMBUSTION PHENOMENA

Semiannual Technical Progress Report
for the Period January 1, 1992 - June 30, 1992

by

Michael L. Swanson, Research Engineer
Michael D. Mann, Research Supervisor
James E. Tibbetts, Research Associate

Energy and Environmental Research Center
University of North Dakota
Box 8213, University Station
Grand Forks, ND 58202-8213

Technical Monitor: Leland Paulson

for

U.S. Department of Energy
Morgantown Energy Technology Center
P.O. Box 880
3610 Collins Ferry Road
Morgantown, WV 26507-0880

July 1992

Work Performed Under Cooperative Agreement No. DE-FC21-86MC10637

TABLE OF CONTENTS

| | <u>Page</u> |
|---|-------------|
| LIST OF FIGURES | ii |
| LIST OF TABLES | iii |
| 1.0 INTRODUCTION | 1 |
| 2.0 GOALS AND OBJECTIVES | 2 |
| 2.1 Three-Year Project Objectives | 3 |
| 2.2 Sixth-Year Objectives | 4 |
| 3.0 PROJECT DESCRIPTION | 6 |
| 3.1 One-Million Btu/Hr Gas Turbine Combustor | 6 |
| 3.2 High-Temperature, High-Pressure Cyclone | 9 |
| 3.3 Pressurized Drop-Tube Furnace | 9 |
| 3.4 High-Pressure Atomization Spray Chamber | 15 |
| 3.5 Advanced Inorganic Analysis Techniques | 18 |
| 3.5.1 SEM Techniques | 18 |
| 3.5.2 Sintering Behavior | 22 |
| 3.5.3 XRF/XRD | 23 |
| 3.5.4 The Chemical Fractionation Technique | 23 |
| 3.5.5 Surface Science | 23 |
| 3.6 Determination of Deposit Strengths | 24 |
| 4.0 RESULTS AND ACCOMPLISHMENTS | 24 |
| 4.1 Fuel Preparation and Analyses | 24 |
| 4.2 Coal-Water Fuel Atomization | 28 |
| 4.3 PDTF Combustion Testing With Beneficiated Fuels | 29 |
| 5.0 CONCLUSIONS AND FUTURE PLANS | 38 |
| 6.0 REFERENCES | 39 |

LIST OF FIGURES

| <u>Figure</u> | | <u>Page</u> |
|---------------|--|-------------|
| 1 | Schematic of 1-MM Btu/hr gas turbine simulator | 7 |
| 2 | Photograph of 1-MM Btu/hr gas turbine simulator | 8 |
| 3 | Design of HTHP cyclone for testing in 1-MM Btu/hr gas turbine simulator | 10 |
| 4 | Photography of HTHP cyclone in exit of lean combustion zone of 1-MM Btu/hr gas turbine simulator | 11 |
| 5 | Pressurized drop-tube furnace process schematic | 12 |
| 6 | Furnace assembly in PDTF vessel | 13 |
| 7 | Photograph of PDTF pressure vessel | 14 |
| 8 | Photograph of PDTF translating mechanism | 15 |
| 9 | Schematic of PDTF sampling probe with interchangeable tips | 16 |
| 10 | Schematic of coal feeder for pressurized drop-tube furnace | 17 |
| 11 | Photograph of pressurized spray chamber | 19 |
| 12 | Deposit-strength measuring apparatus | 25 |
| 13 | Weight percent of total elements in each size fraction for Spring Creek coal combustion testing at 100 psi with and without Kaolin addition | 32 |
| 14 | Weight percent of total elements in each size fraction for Spring Creek Coal combustion testing at atmospheric pressure with and without kaolin addition | 32 |
| 15 | Photograph of flakes of final filter cake | 34 |
| 16 | High-magnification photograph of final filter cake. | 34 |

LIST OF TABLES

| <u>Table</u> | <u>Page</u> |
|--|-------------|
| 1 Proximate and Ultimate Analyses of Fuels Tested | 26 |
| 2 X-Ray Fluorescence Analysis of LRC Fuels Tested in Turbine Program: High-Temperature Ash Results (% of ash, SO ₃ -free) . . . | 26 |
| 3 Chemical Fractionation Results of Raw Spring Creek Coal | 27 |
| 4 Chemical Fractionation Results of Hydrothermally Treated Spring Creek Coal | 27 |
| 5 Summary of CCSEM Results for PC/AC/HWD Spring Creek Fuel | 28 |
| 6 Summary of CCSEM Results for HWD/Micronized Spring Creek Fuel Produced for Allison Gas Turbines | 29 |
| 7 Summary of CCSEM Results for Raw Spring Creek Fuel | 30 |
| 8 CCSEM Analysis with Image Analysis for Allison HWD/Micronized Spring Creek Fuel | 31 |
| 9 CCSEM Analysis with Image Analysis for Raw Spring Creek | 33 |
| 10 Operating Conditions and Results from Shakedown Combustion Tests Using Allison Fuel Spring Creek Coal | 35 |
| 11 Operating Conditions and Results from Shakedown Combustion Tests Using Allison Fuel Spring Creek Coal | 36 |
| 12 Operating Conditions and Results from Fly Ash Combustion Tests Using Allison Fuel Spring Creek Coal | 37 |
| 13 Operating Conditions from Fly Ash Combustion Tests Using PC/AC/HWD/Micronized Spring Creek Coal | 38 |
| 14 Operating Conditions and Results from Fly Ash Combustion Tests Using Raw Spring Creek Coal and Spring Creek Coal Mixed with Kaolin for Alkali Gettering | 40 |
| 15 SEMPC and XRD Analyses--Multicyclone Fly Ash Samples | 41 |
| 16 SEMPC and XRD Analyses--Multicyclone Fly Ash Samples Run APSPC040 | 42 |
| 17 SEMPC and XRD Analyses--Multicyclone Fly Ash Samples Run SPCRK041 | 43 |
| 18 SEMPC and XRD Analyses--Multicyclone Fly Ash Samples Run SPCRK042 | 44 |
| 19 SEMPC and XRD Analyses--Multicyclone Fly Ash Samples Run SPCRK043 | 45 |
| 20 SEMPC and XRD Analyses--Multicyclone Fly Ash Samples Run AFSPC045 | 46 |

TURBINE COMBUSTION PHENOMENA

1.0 INTRODUCTION

Under DOE sponsorship coal-water slurry fuels have been investigated as fuels for gas turbine engines for several years, but the major technical problems still inhibiting commercialization are deposits on the pressure and suction sides of the turbine blades which reduce the gas flow area and turbine efficiency; acceptable coal burnout, given the short residence time inherent with gas turbine engines; corrosion of turbine blades by condensed alkali sulfates; erosion of turbine blades and other components by ash particles entrained in the products of combustion; and control of NO_x , SO_2 , and particulate emissions. The release of certain mineral matter species found in both raw and beneficiated coals can lead to ash deposition on surfaces, regardless of the ash content of the fuel. This deposition can lead to corrosion on and metal loss of critical turbine components and, ultimately, to derating, unavailability, or catastrophic failure of the power generation system. Alkali metals and sulfur, existing as impurities in coal, have been identified as key components in the initiation of deposition and the onset of corrosion.

Until the last six years, low-rank coals (LRCs) were not considered as potential fuels for gas turbine engines because of their high intrinsic moisture levels. It is extremely difficult to prepare a pumpable slurry of as-mined lignite with a dry solids loading over 35 wt% due to the high moisture levels in LRCs. However, with the advent of the University of North Dakota's Energy and Environmental Research Center's (EERC's) hydrothermal treatment process, micronized lignite slurries have been produced with a solids loading up to 50% and a heating value over 6000 Btu per pound of slurry (1,2). Subbituminous coals also respond very well to hydrothermal treatment and produce higher quality slurries. Availability of a slurry with a high enough fuel value to sustain combustion makes it possible to take advantage of the desirable characteristics of low-rank coals, namely, the higher reactivity of its nonvolatile carbonaceous components. Thus a low-rank coal slurry should require less residence time in the gas turbine combustor for complete combustion or, inversely, the coal would not have to be micronized as finely to achieve >99% burnout, thereby reducing fuel preparation costs. Estimates of the process have indicated that a minemouth process plant in the Powder River Basin can produce a LRCWF at around \$1.50/MM Btu, including coal costs (3). Another potential advantage of low-rank coal slurries is their nonagglomerating tendency relative to bituminous slurries, reducing the importance of atomization to very fine droplet sizes.

During the Turbine Combustion Phenomena project, seventeen successful combustion tests using CWF were completed. These tests included seven tests with a commercially available Otisca Industries-produced, Taggart seam bituminous fuel and five tests each with physically and chemically cleaned Beulah-Zap lignite and a chemically cleaned Kemmerer subbituminous fuel. Analyses of the emission and fly ash samples highlighted the superior burnout experienced by the LRCWFS as compared to the bituminous fuel even under a longer residence time profile for the bituminous fuel. While the LRC fuels are experiencing better burnout than the bituminous fuels, it is possible that differences in slurry rheology (and, therefore, in atomization) might account for some of the difference in the observed burnout rather than differences in

fuel reactivity. The LRC fly ash showed a decrease in particle size as compared to the starting fuel, while the bituminous fuel showed an increase in particle size as compared to the starting fuel. These particle-size analyses provide some evidence of low-rank coals' nonagglomerating properties as compared to bituminous fuels.

Statistical analysis of the carbon burnout data generated in a series of parametric combustion tests generated simple models to predict the carbon burnout achievable under a given range of operating conditions. These models indicate that fuel type has a significant effect on the measured carbon burnout. The LRC fuels have high carbon burnouts (97.5% to 98.7%) and appear to be relatively unaffected by other operating parameters; however, the bituminous fuel was significantly affected by combustion air temperature, atomizing air-to-fuel ratio, and fuel firing rate. In this model, bituminous fuel carbon burnouts comparable to those of the LRC fuels can be achieved, but only under the most optimum conditions.

As might be expected with the relatively high ash in the LRC fuels and lower ash fusion temperatures, significant ash deposition and slagging occurred in the turbine simulator. The XRD analysis suggests that the residual magnetite left from the physical cleaning process remains as magnetite in the reducing atmosphere of the rich zone, but is converted to hematite when it reaches the highly oxidizing atmosphere encountered in the lean combustion zone. The composition of the constituents in the ash does not indicate the preferential deposition of any component in a single area of the turbine. Material balances indicate that the Beulah Zap lignite fuel had a much higher deposition potential as demonstrated by high levels (approximately 70 wt%) of ash recovered in the combustor. The Kemmerer fuel also showed higher deposition levels than the Otisca fuel, with approximately 12-13 wt% of the ash being retained in the combustor. With the Otisca fuel combustion tests approximately 8 wt% of the ash was retained in the combustor, while over 40 wt% of the Otisca fly ash was recovered in the cyclone pot. This is probably the result of the cyclone ash containing high levels of carbon (60% or greater); thus a large percentage of the fine mineral grains is still tied up in the char cenospheres and has not been released from the char particle where it could contact internal surfaces to form deposits.

2.0 GOALS AND OBJECTIVES

The overall objective of this research is to continue to expand the database on the effects of low-rank coals' unique properties on their combustion behavior in pressurized combustion systems, such as gas turbine engines. Research will be directed toward understanding the properties of LRC fuels which affect ignition and burn times, combustion efficiency, vaporization and deposition of inorganics, and the erosion of critical gas turbine components. Special emphasis will be placed on an investigation of LRC high-shear rheology and its effect on atomization and combustion behavior, an evaluation of LRCs' nonagglomerating properties, an investigation of particulate hot-gas cleanup techniques, and inorganic transformations/alkali vaporization using a pressurized drop-tube furnace.

2.1 Three-Year Project Objectives

- Task A **Revise Technology and Market Assessment.** This literature review will enable EERC personnel to assess the current status of coal-fired gas turbine research to determine what recent advances have been made by other researchers. This effort will build upon the technology and market assessment made at the start of this program. This task is to be performed in Year Four.
- Task B **Characterization of LRCs' Atomization Properties.** This task will examine the pressurized atomization characteristics of recently produced LRC fuels with a Malvern 2600 particle-size analyzer and still photography in a pressurized spray chamber constructed at the EERC. The combustion behavior of the previous fuels tested in the spray chamber and new fuels produced for the turbine project will be evaluated under similar air-to-fuel and pressure ratios in the gas turbine simulator. This task will also look at different atomizer types in an effort to minimize spray droplet size distributions and increase combustion performance for a given rheology and atomizing air-to-fuel ratio.
- Task C **Evaluation of LRC Fuel Agglomeration.** The objective of this task is to evaluate the agglomerating or nonagglomerating tendencies of LRC fuels by providing optical access for an Insitec particle counter, sizer, and velocimeter (PCSV) at various positions along the axis of a pressurized drop-tube furnace recently constructed at the EERC. Thus products of combustion (POC) particle-size distributions as a function of residence time and the starting particle-size distribution and droplet size can be measured to determine if the smaller particle-size distributions found in the LRC fly ash are the result of a gradual burnout of slurry droplet agglomerates or the result of agglomerate disintegration into its original particle-size distribution due to the high thermal friability of LRC fuels.
- Task D **Investigation of Particulate Hot-Gas Cleanup Systems.** The objective of this task is to evaluate potential hot-gas particulate cleanup techniques as to their relative probability of success and test the best two or three systems in the turbine simulator. This task will include a technology assessment that will build upon a previous literature search performed on hot-gas cleanup techniques. These techniques could include, but would not be limited to, ceramic cross-flow filters and filter candles, nested fiber filters, cyclones, and HTHP Electrostatic precipitators (ESPs). The HTHP cyclone work started in Year Four will be continued in the Year Five Hot-Gas Cleanup program. This work involves tests with various CWFs' in an effort to reduce the fly ash particle-size distribution entering the deposition section of the turbine simulator to 95% less than 5 microns in order to limit the amount of particle impaction on the turbine blades.
- Task E **Ash Transformation Studies.** The objective of this task is to investigate the ash transformations experienced by mineral matter in beneficiated low-rank coal fuels. Very little research to date has investigated the effects of pressure and coal beneficiation on the reaction pathways taken by the mineral matter present in LRC fuels.

These transformations should be dependent on the cleaning techniques used and the level of cleaning achievable on the various coal types. Mineral matter transformations of beneficiated LRC under turbine operating conditions will be investigated in a pressurized drop-tube furnace recently constructed at the EERC. This drop-tube furnace will be capable of combusting both slurry droplets and coal particles. The effects of residence time, temperature, pressure, atmosphere, and gas/fuel flow rates can be varied to examine their effects on ash transformations and carbon burnout. The drop tube will also provide carbon burnout as a true function of residence time given the laminar gas flow. The effects of deposition probe shape and temperature and the approaching gas velocity on the measured deposition rates can also be investigated. Another advantage of the pressurized drop-tube furnace is the small quantities of fuel (up to 1.0 g/min) needed to conduct extensive deposition and burnout testing as compared to the turbine simulator (approximately 150 lb/hr). High ash fusion temperature fuels are needed under the assumption that low melting temperature ashes will stick to the cyclone wall or the ceramic material and will not be easily removed or cleaned from the hot-gas cleanup device. Technical work in this task for Year Six will consist of two tasks involving combustion tests using fuels beneficiated to various levels and fuels doped with additives selected for their ability to decrease deposition potential. These tests will measure the effect these additives have on the sticking coefficient and deposition rates measured at conditions similar to those utilized in previous deposition tests.

Task F Investigation of Slagging Combustor Design. Should concurrent beneficiation of LRC studies at the EERC indicate that acceptable ash levels and chemistry not be achievable, a vertically fired combustion zone would be built to replace the horizontally fired rich combustion zone on the current turbine simulator. This modification would enable the combustor to operate in a slagging combustor mode versus the current nonslagging combustor mode. Work on this task would be dependent on the results of the work in progress and would be subject to DOE approval.

Task G Baseline Combustion Test with Spring Creek Fuel Utilized in GM Allison Combustion Tests

The production of several barrels of minimally cleaned Spring Creek coal for the Turbine Combustion Phenomena program was added to the large production runs performed for GM Allison. A combustion test will be used to establish a performance baseline in the 1-MM Btu/hr gas turbine simulator for the Powder River Basin coal used by GM Allison in its direct coal-fired gas turbine system. Thus future comparisons of the two combustion rigs can be made, especially the performance of hot-gas cleanup devices in these systems.

2.2 Sixth-Year Objectives

Task A Revise Technology and Market Assessment

Performed in the fourth year.

Task B Characterization of LRCs' Atomization Properties

Ongoing with Year Five carryover funds.

Task C Evaluation of LRC Fuel Agglomeration

Unable to perform due to inoperability of Insitac particle sizer, counter, and velocimeter (PSCV).

Task D Investigation of Particulate Hot-Gas Cleanup Systems

The performance of long-term hot-gas cleaning tests should be performed on the PDTF (if availability permits) due to the lower cost of maintaining long test durations in this system. Parameters of interest are alkali levels, operating temperatures and pressures, particulate loading, and number of cleaning cycles.

Task E Ash Transformation Studies

Technical work in this task for Year Six will consist of two tasks involving combustion tests using fuels beneficiated to various levels and fuels doped with additives selected for their ability to increase ash fusion temperatures. These tests will measure the effect these additives have on the sticking coefficient and deposition rates measured at conditions similar to those utilized in previous deposition tests. These tests will determine an additive that hopefully will provide a fuel with a nonmolten fly ash without significantly increasing the total fly ash concentration in the flue gas. These selected doped fuels would be suitable for tests in both the HTHP cyclone and ceramic filter apparatus.

Task E-1 Ash Transformation Studies for Beneficiated LRC Fuels

The objective of this task is to investigate the ash transformations experienced by mineral matter in beneficiated low-rank coal fuels. Very little research to date has investigated the effects of pressure and coal beneficiation on the reaction pathways taken by the mineral matter present in LRC fuels. These transformations should be dependent on the cleaning techniques used and the level of cleaning achievable on the various coal types. Cleaning techniques which will be investigated are heavy media physical cleaning, an acid-leaching chemical-cleaning technique, hydrothermal treatment, and oil agglomeration. Mineral matter transformations of beneficiated LRC under turbine operating conditions will be investigated in a pressurized drop-tube furnace recently constructed at the EERC. The effects of residence time, temperature, pressure, atmosphere, and gas/fuel flow rates can be varied to examine their effects on ash transformations and carbon burnout. The drop tube will also provide carbon burnout as a true function of residence time given the laminar gas flow. The effects of deposition probe shape and temperature and the approaching gas velocity on the measured deposition rates can also be investigated.

Task E-2 PDF Additive Testing for Improved Ash Characteristics

Alkali gettering or additives which tie up the volatile and molten species in the mineral matter is needed to protect downstream hot-gas cleanup devices and the turbine blades themselves. High ash fusion temperature fuels are needed under the assumption that low melting temperature ashes will stick to the ceramic material and will not be easily removed or cleaned from the hot-gas cleanup device. Other research needs were identified as characterizing the trace elements in the gas turbine (GT) flue gas.

Task F Investigation of Slagging Combustor Design

No technical work in this task will be performed in Year Six. If coal ash properties dictate, construction of a first-stage slagging combustor would begin in subsequent years.

Task G Baseline Combustion Test with Spring Creek Fuel Utilized in GM Allison Combustion Tests

The production of several barrels of minimally cleaned Spring Creek coal for the Turbine Combustion Phenomena program was added to the large production runs performed for GM Allison. A combustion test will be used to establish a performance baseline in the 1-MM Btu/hr gas turbine simulator for the Powder River Basin coal used by GM Allison in its direct coal-fired gas turbine system. Thus future comparisons of the two combustion rigs can be made, especially the performance of hot-gas cleanup devices in these systems.

3.0 PROJECT DESCRIPTION

3.1 One-Million Btu/Hr Gas Turbine Combustor

To meet the objectives of the initial program, a pressurized combustion vessel was built to allow the operating parameters of a direct-fired gas turbine combustor to be simulated. One goal in building this equipment was to design the gas turbine simulator as small as possible to reduce both the quantity of test fuel needed and the test fuel preparation costs, while not undersizing the combustor such that wall effects would have a significant effect on the measured combustion performance. Based on computer modeling, a rich-lean, two-stage nonslagging combustor has been constructed to simulate a direct-fired gas turbine. This design was selected to maximize the information that could be obtained on the impact of the unique properties of low-rank fuels and various hot-gas cleanup techniques on the gas turbine combustor and its turbomachinery.

A short description of the gas turbine simulator is given here; a more detailed description is given elsewhere (4-6). Figure 1 is a schematic of the 1-MM Btu/hr gas turbine combustor showing its internal design. Figure 2 is a photograph of the 1-MM Btu/hr gas turbine combustor. The head section of the turbine has an interchangeable, horizontal, flat-bladed air swirler for controlling the primary air-fuel spray and developing a recirculation zone in the rich combustion zone. A Delavan Swirl-Air nozzle with a 50° spray angle

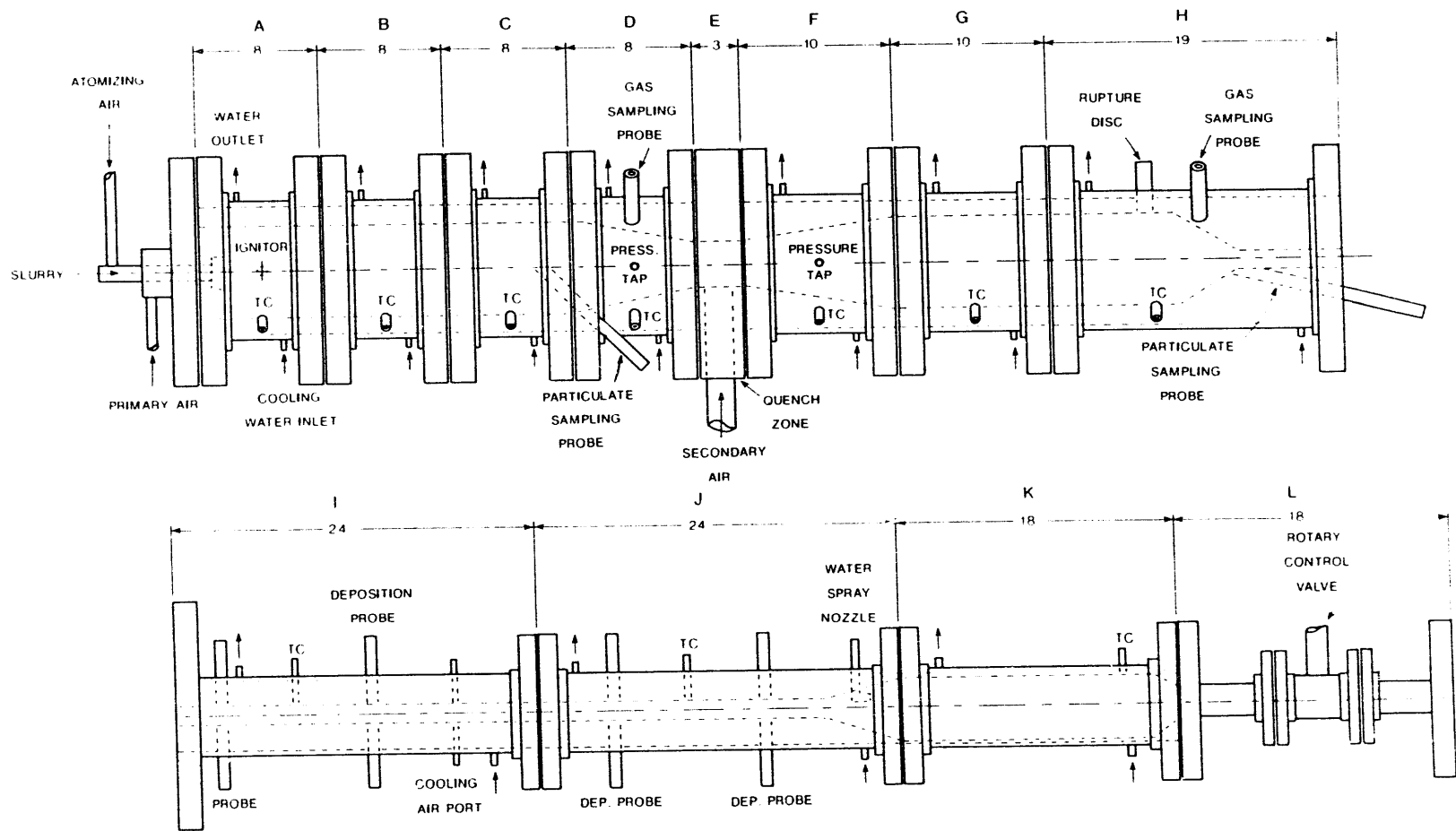


Figure 1. Schematic of 1-MM Btu/hr gas turbine simulator.

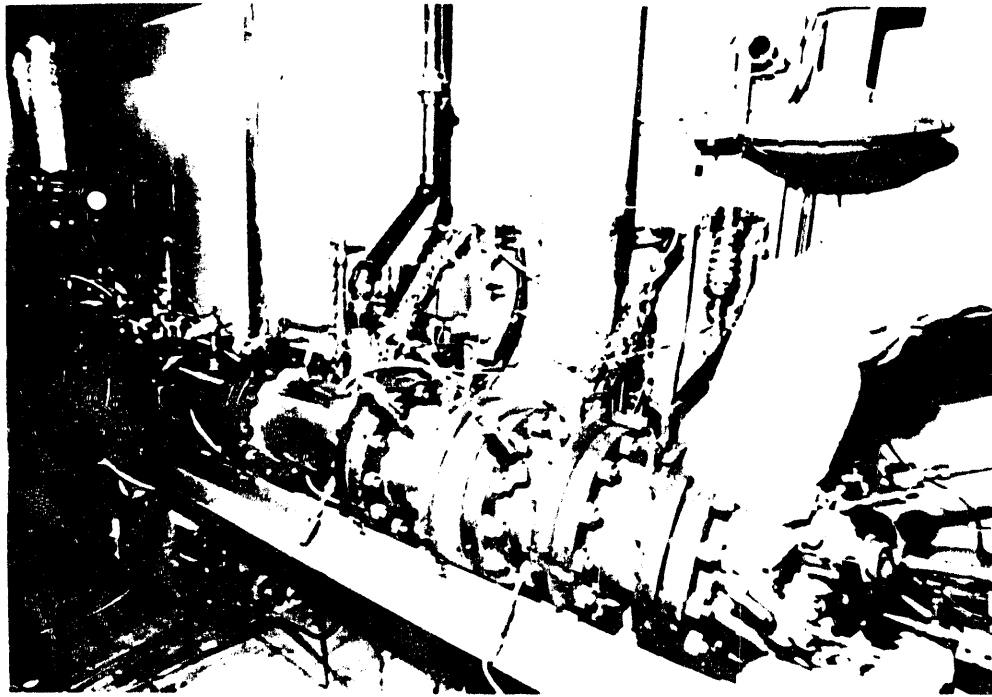


Figure 2. Photograph of 1-MM Btu/hr gas turbine simulator.

is currently used as the atomizer. The pressurized combustion vessel itself is comprised of several short sections of refractory-lined stainless steel pipe. These sections are water-jacketed to provide cooling of the external pressure vessel wall. This modular design allows the length of the combustion zones to be varied. The removal of some of these modules allows the effect of residence time to be investigated under similar flow conditions.

The quench zone of the turbine simulator was designed to promote rapid mixing of the secondary air with the POC exiting the rich combustion zone, thus minimizing the occurrence of localized "hot spots" and the formation of thermal NO_x . A rotary control valve and a high-temperature-guided seat control valve are used to control the flow of combustion air entering the air preheater and the distribution of air between the rich and lean zones, respectively. The combustor is designed to operate at pressures up to 250 psig and a lean zone exit temperature of 2000°F.

A reduced flow area in the deposition section is used to increase the gas velocities up to those typically seen in the expander section of a gas turbine (400 to 800 ft/sec). Four air-cooled probes with various contact angles were machined from thick-walled high-temperature alloy tubing and were installed to simulate the leading edge of turbine blades. Additional cooling air was added after the first two probes to cool the exit gas stream up to 200°F, such that gas temperature as well as metal temperature can be investigated for their effects on deposition/erosion/corrosion (DEC). A spray water quench zone is located after the deposition section to spray high-pressure water into the combustion gases to cool the gases before passing them

through the rotary control valve used to back pressure the turbine simulator. A natural gas-fired fluidized-bed preheater is used to preheat the high-pressure combustion air to temperatures as high as 1000°F. Combustion efficiencies of the test fuels fired in the turbine simulator are calculated from gas and isokinetic particulate samples taken from both the rich and lean zones of the combustor.

3.2 High-Temperature, High-Pressure Cyclone

Figure 3 is a drawing showing the design of the high-temperature, high-pressure (HTHP) cyclone which has been inserted in the turbine simulator combustion system located at the EERC. This cyclone is fabricated from 8-inch schedule 40 pipe welded to form an off-center tee. This pipe is water-jacketed to keep the metal wall temperatures low. As shown in Figure 3, the cyclone dimensions are cast in refractory inside the tee. This cyclone replaced the last section of the lean combustion zone shown in Figure 1. Figure 4 shows the HTHP cyclone inserted in the gas turbine simulator combustion system. Openings have been included in the vessel walls for measuring the inlet and outlet combustion gas temperatures and pressures. In addition, openings have also been included for taking upstream particulate samples, while an existing port will allow downstream particulate samples to be collected for measuring the cyclone efficiency. A second opening was added for a water-jacketed and sealed baroscope viewing system which is currently being constructed. This baroscope will allow the flame quality and stability to be monitored during combustion tests.

3.3 Pressurized Drop-Tube Furnace

The emergence of advanced coal combustion technologies such as coal slurry-fired gas turbines requires fundamental knowledge of the fuel combustion processes at elevated pressures. Of critical importance is the basic combustion kinetics and the fate of coal mineral matter in such systems.

To address these issues, a pressurized drop-tube furnace was also constructed. The pressurized drop-tube furnace (PDTF) is capable of operating under the following conditions:

| | |
|-----------------|--------------------------------|
| Temperature: | ambient to 2732°F (1500°C) |
| Pressure: | ambient to 300 psia (20.4 atm) |
| Oxygen: | 0-20 mole% |
| Gas Flow: | 0 to 7.8 scfm (220 L/min) |
| Residence Time: | 0 to 5.0 sec |

- Optical access at any residence time
- Provision for char and ash collection
- Provision for ash deposition studies

The design of the PDTF incorporates several novel features which allowed the design goals to be met. A drawing of the PDTF facility is given in Figure 5. The entire PDTF is constructed of standard 24" and 6" flanged pipe sections. The large pressure vessel contains the furnace sections of the PDTF as shown in Figure 6. Figure 7 is a photograph of the PDTF pressure vessel. The walls of the vessel are water-cooled to dissipate the heat from the furnaces. A preheater and two furnace sections are located above the

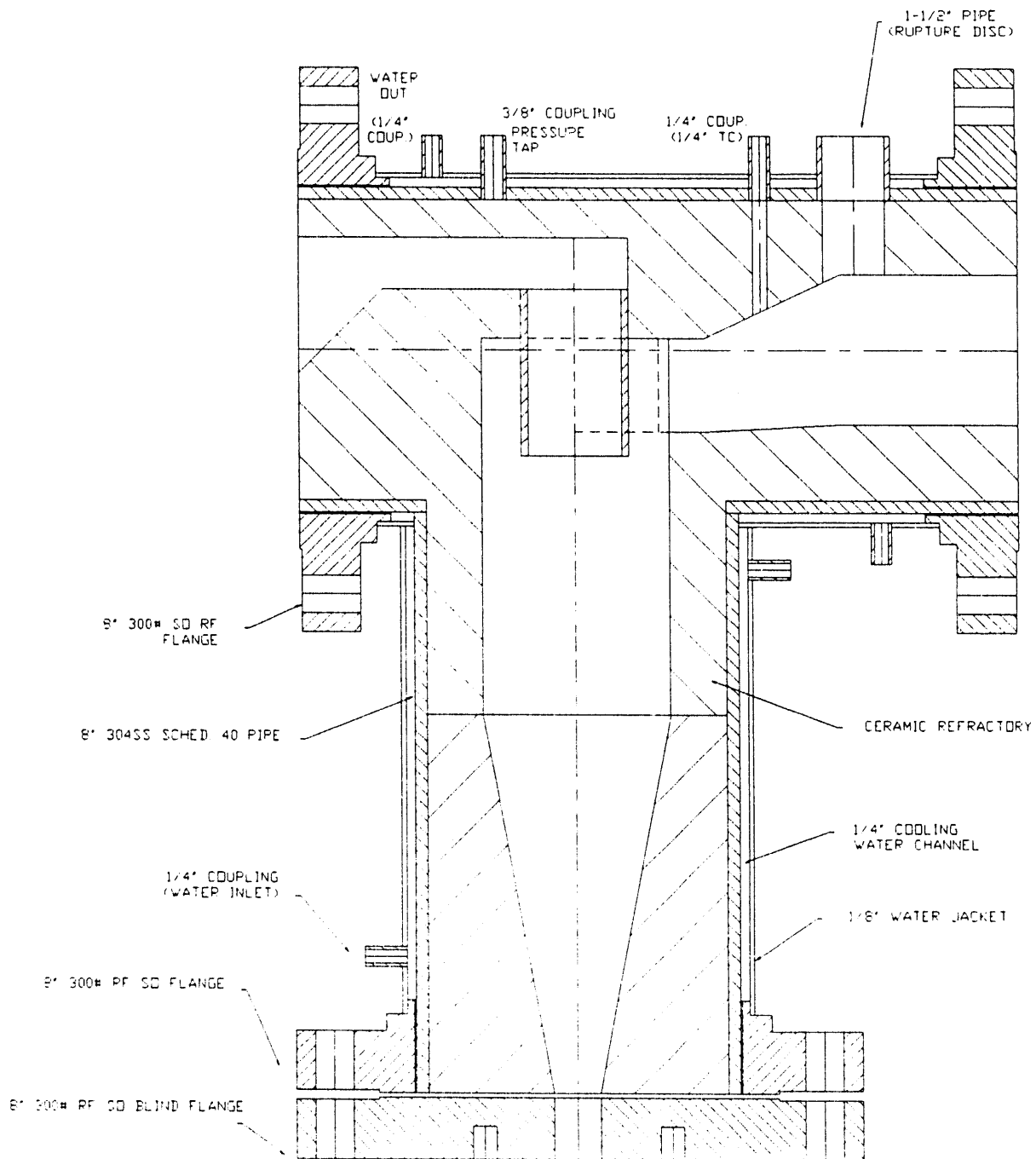


Figure 3. Design of HTHP cyclone for testing in 1-MM Btu/hr gas turbine simulator.

optical sight ports, and one furnace is located below the optical sight ports to reduce the temperature gradient across the optical access section. Optical access is provided by four 3" diameter ports in the pressure vessel. Electrical power is supplied to the furnaces by electrical feed through the terminals in the bottom blind flange of the pressure vessel.



Figure 4. Photography of HTHP cyclone in exit of lean combustion zone of 1-MM Btu/hr gas turbine simulator.

Above the large pressure vessel shown is the injector section containing the injector assembly. The injector is a 1-inch-diameter water-cooled probe sheathed in high-temperature insulation. Figure 8 is a photograph showing the translating mechanism used for raising and lowering the injector into the ceramic tube inside the furnace assembly. The injector may be retracted completely out of the furnace when not in use or may be lowered into the furnace to give the desired residence time between 0 and 5.0 seconds. Small viewports in the pipe crosses at the bottom and top of the injector section allow visual inspection of the probe and the sample-feeding behavior.

Below the large pressure vessel is a sampling probe assembly and translation mechanism. The sampling probe may be raised to the level of the optical access ports and retracted completely from the furnace for the removal of sample deposits or when not in use. Two pipe crosses with small sight ports allow inspection of the collection probe operation, and the removal of a blind flange provides access for the removal of sample deposits. The sampling probe tip is interchangeable to allow deposition or fly ash samples to be collected without removing the entire sample probe. Figure 9 shows the construction details of the sampling probe.

The sample feeder assembly is a blank flanged 6" pipe cross pressurized to slightly above the furnace pressure with gas connections to the furnace assembly. Figure 8 also shows the sample feeder pressure vessel located next to the sample injector translating mechanism. Figure 10 is a schematic of the coal feeder used in the PDTF. The design allows the actual sample feeder to be constructed of lightweight material, since it does not have to withstand

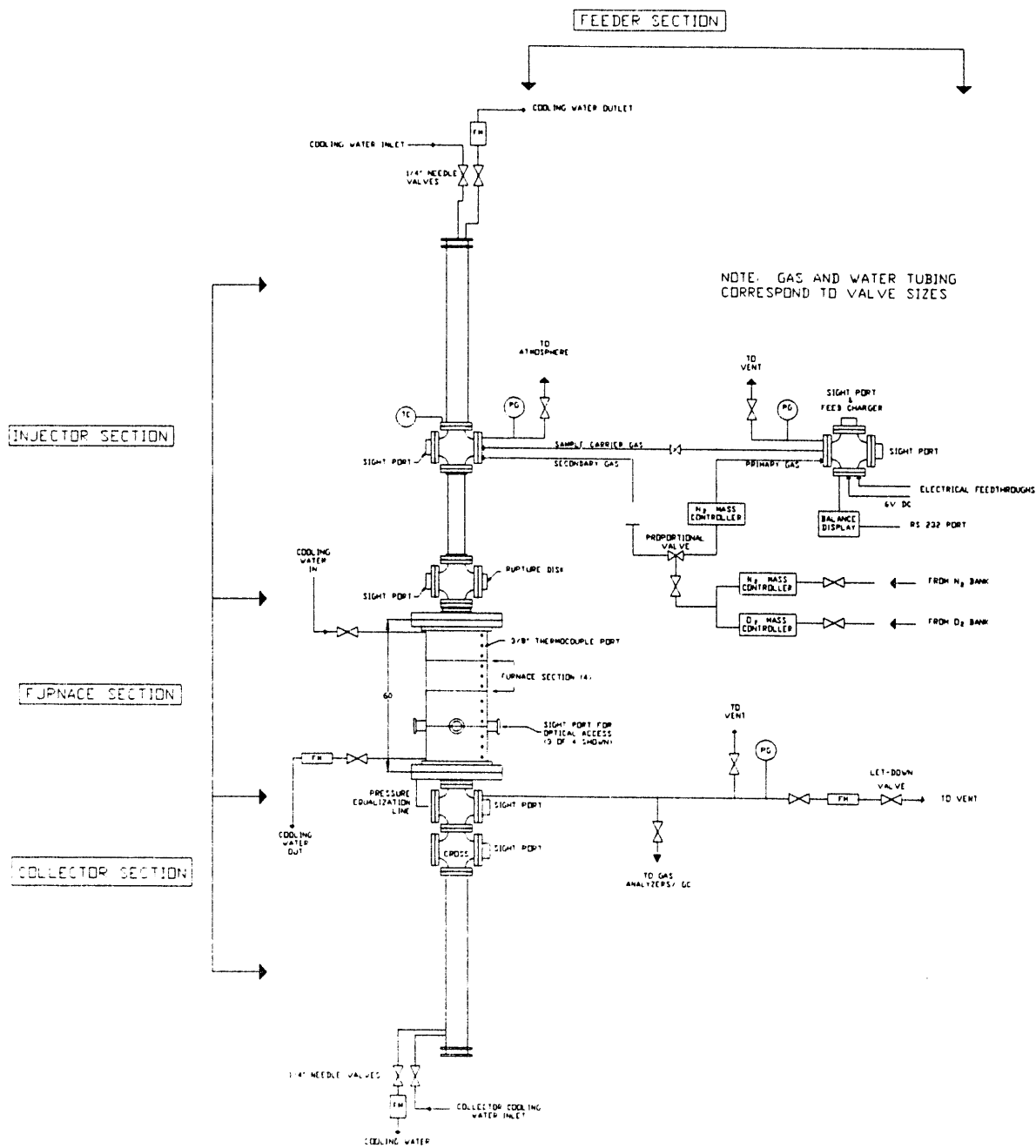


Figure 5. Pressurized drop-tube furnace process schematic.

more than slight pressure differentials. A small sight port allows inspection of the feeder operation, and the removal of a blind flange gives access to the vessel for filling or adjustment of the feeder. The lightweight feeder can then hang from a load cell in the pressure vessel to provide a continuous record of the sample feed rates. The gas composition and flow rate of gas

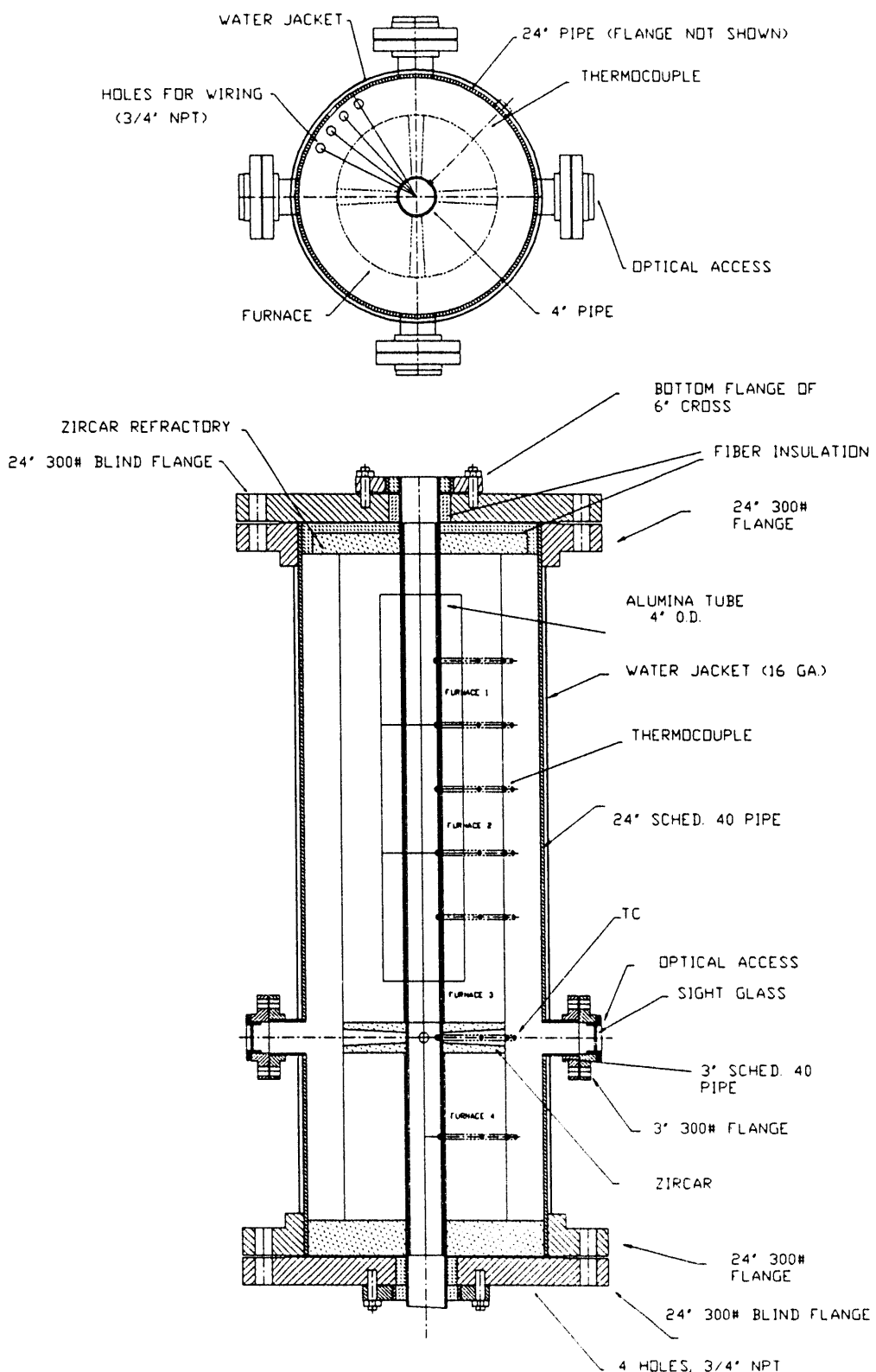


Figure 6. Furnace assembly in PTFE vessel.

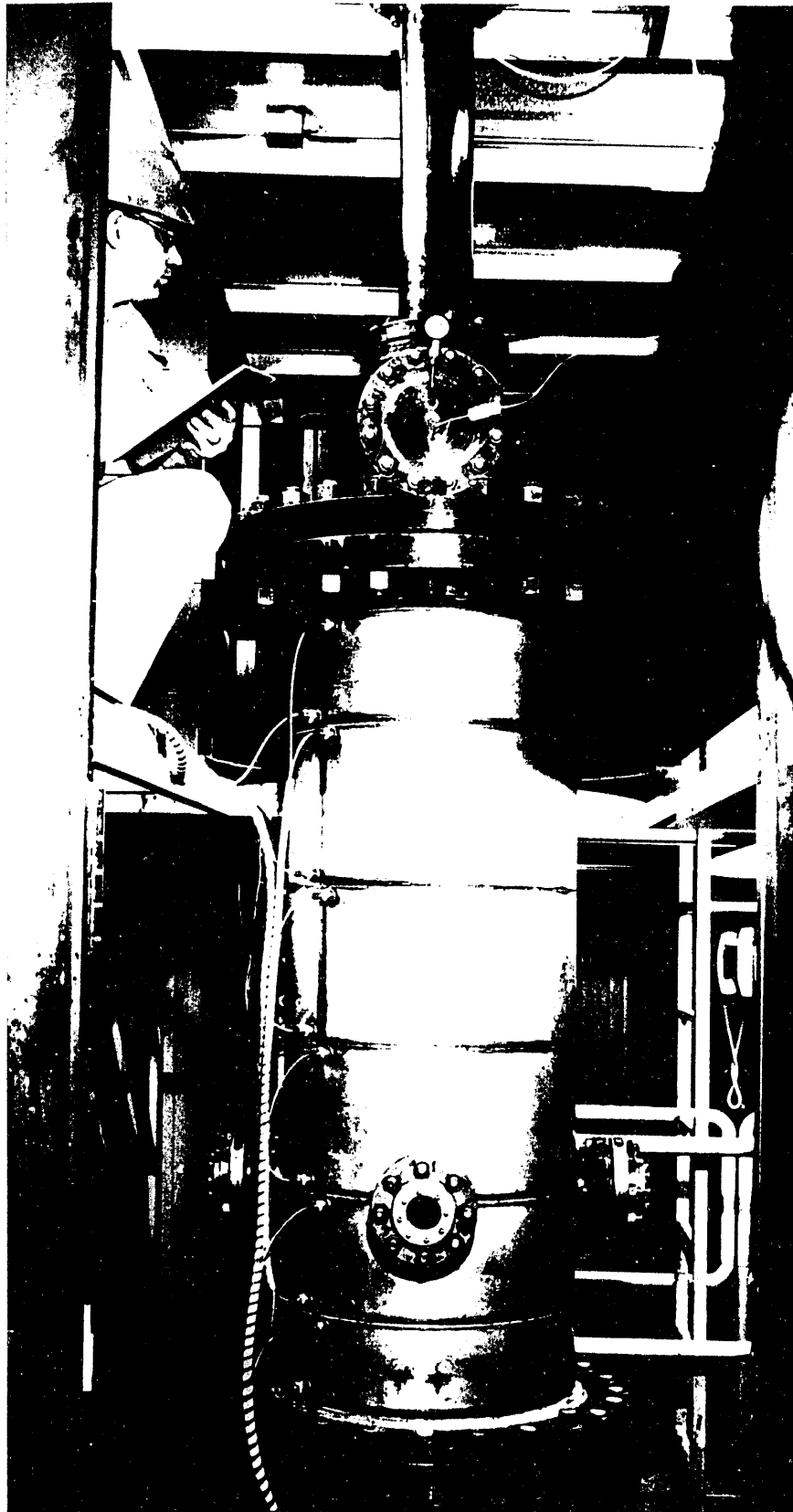


Figure 7. Photograph of PDF pressure vessel.

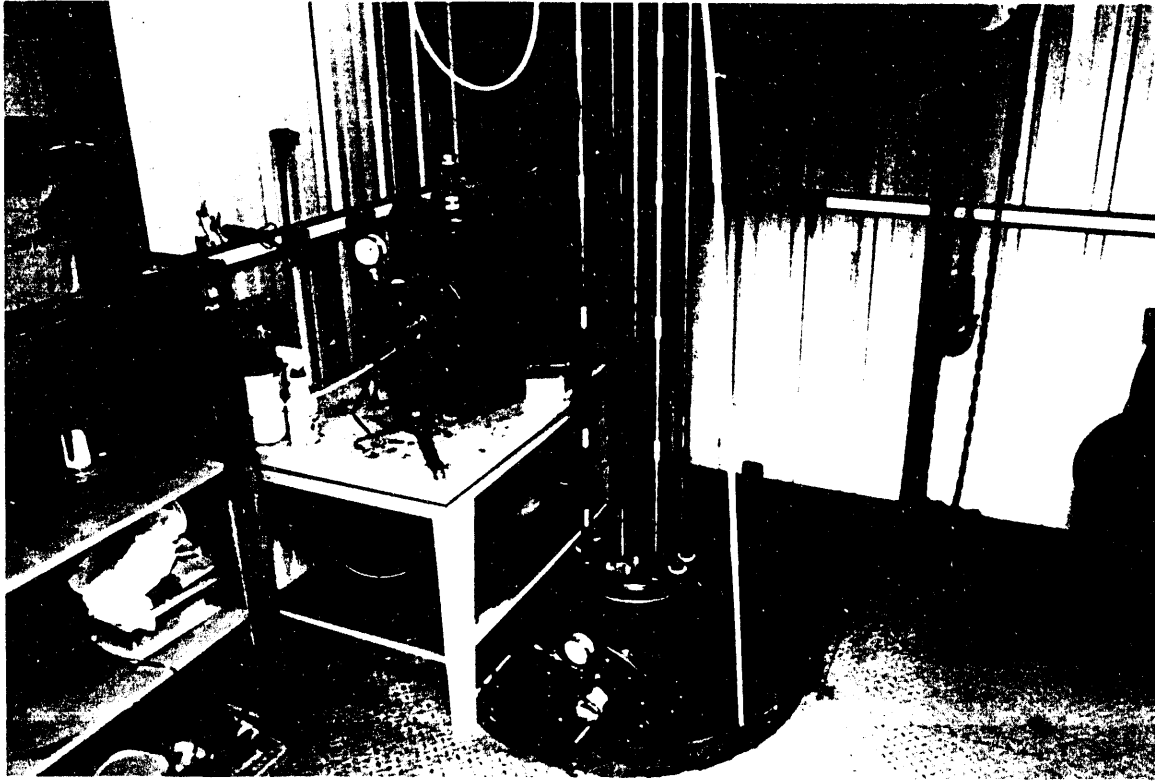


Figure 8. Photograph of PDTF translating mechanism.

into the PDTF is controlled by oxygen and nitrogen mass flow controllers. Gas composition can be controlled between 0-20 mole % at flow rates up to 220 L/min. The furnace pressure is controlled by a letdown control valve at the exit of the furnace.

3.4 High-Pressure Atomization Spray Chamber

An existing pressure vessel has been modified to include observation ports to perform atomization studies under typical turbine operating pressures and air flows. The main objective of this work is to determine if differences in atomization quality account for the improvements in carbon burnout experienced with the LRC fuels. The design of the spray chamber involves an existing 11.25-inch-ID pressure vessel which has been modified to provide optical access perpendicular to the direction of the atomized spray. The optical access consists of two diametrically opposite 3" sight ports for the use of high-speed photography. In addition, a 2" sight port opposite of a 1" NPT port through which a sight pipe can be inserted has also been added. The use of a sight pipe reduces the length of the spray which the Malvern 2600's laser beam must pass through and eliminates the potential for vignetting which could occur if the beam were to pass through the complete spray cone. A honeycomb catalyst support is used as a flow straightener to provide a laminar flow of air around the atomizing nozzle. The height of the atomizer in relationship to the optical ports is adjustable from outside the pressure vessel, thus allowing the atomizer position to be changed during a single atomization test.

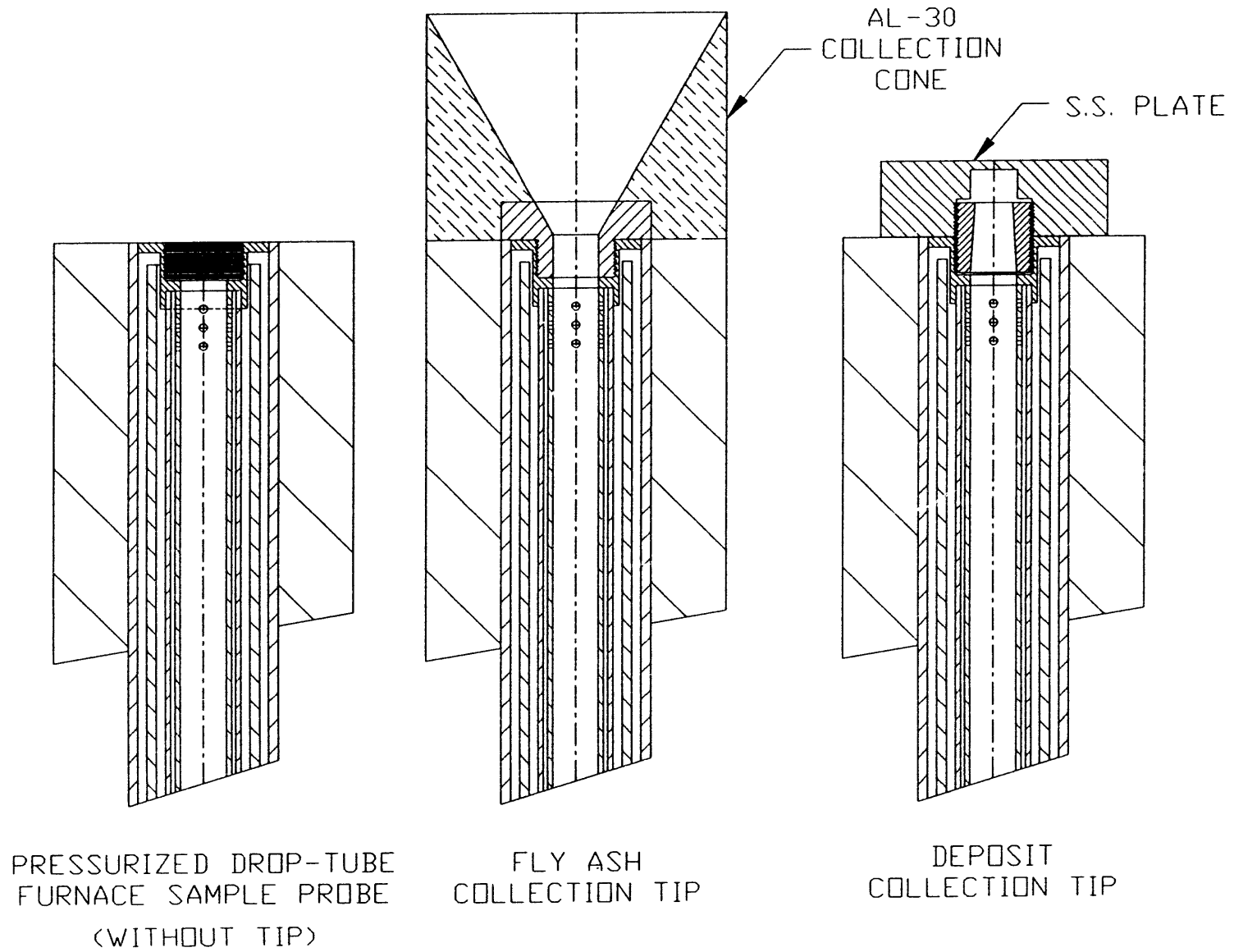


Figure 9. Schematic of PETF sampling probe with interchangeable tips.

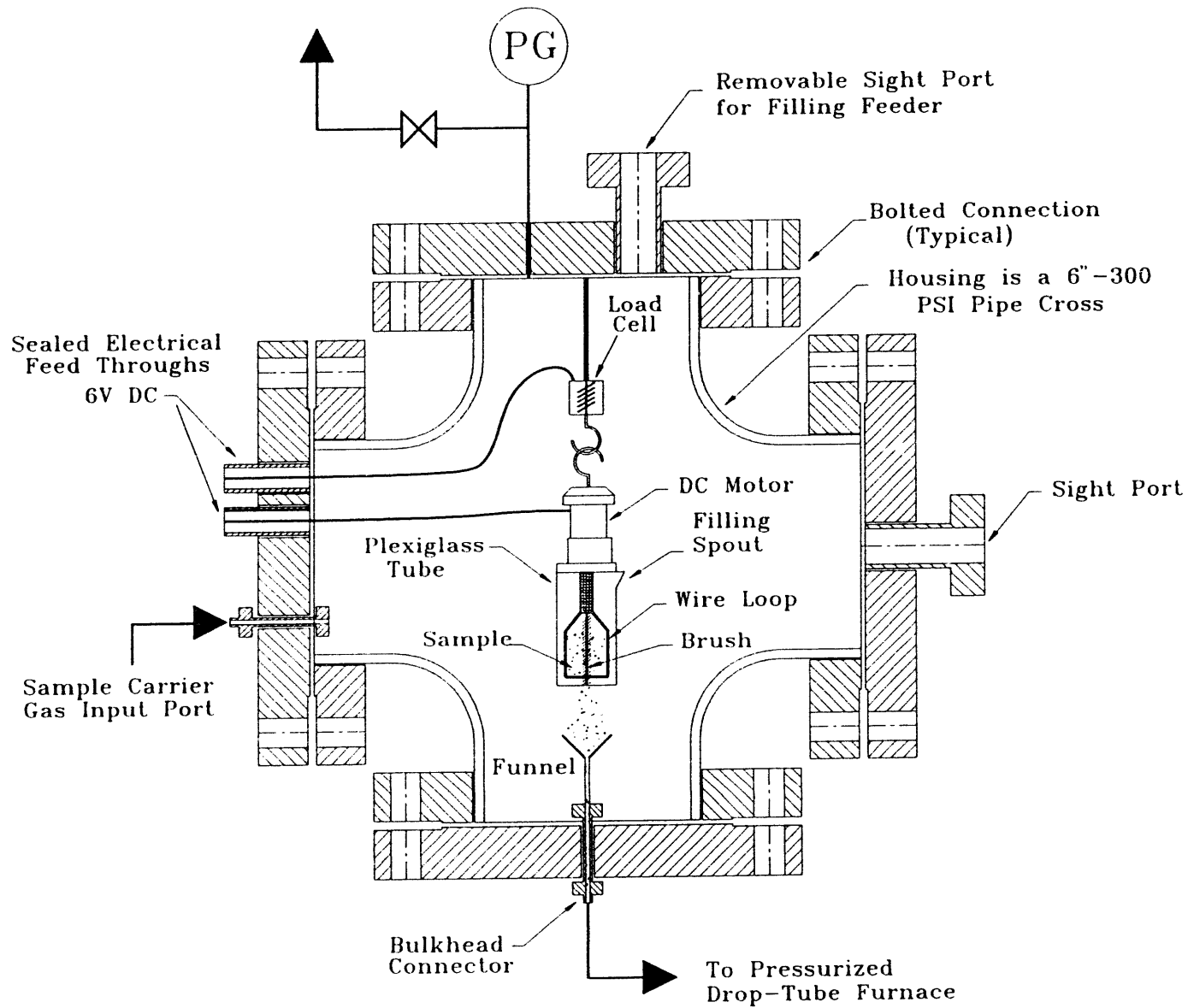


Figure 10. Schematic of coal feeder for pressurized drop tub furnace.

Figure 11 is a photograph of the pressurized spray chamber. The atomized slurry is collected in a funnel at the bottom of the spray chamber where it is drained off to a pressurized separation vessel. Pneumatic control valves are used to control the air flow rate and to back pressure the spray chamber. High-speed photography is accomplished using a high-speed strobe to backlight the slurry droplets during atomization. The use of high-speed photography allows droplet sizes larger than 564 microns (the top size for a Malvern particle-size analyzer with a 300-mm lens) to be detected and also provides information about the spray angle obtained under a given set of operating conditions.

An atomizer has been constructed which allows different types of atomizers to be utilized by simply changing the tip of the atomizer. Commercially available atomizers which can be utilized in the spray chamber are the internal-mixed Delavan Swirl-Air nozzles rated for 1.0 and 2.5 gallons-per-minute (gpm) liquid flow rates and a Delavan external mix atomizing air nozzle (Part #47283-1). The Swirl-Air atomizers are carbide-lined versions to reduce the amount of atomizer tip erosion experienced from the high-velocity CWF passing through the common orifice. The commercially available Parker Hannifan M2 (atmospheric combustion systems) and M6 (for pressurized combustion systems) can also be utilized. The EERC B-II nozzle made in-house for CWF testing in atmospheric combustion systems can also be utilized with large or small diameter orifice tips (0.175 and 0.125" ID).

3.5 Advanced Inorganic Analysis Techniques

Extensive research on the transformations of inorganic and mineral components in coal has been conducted at the EERC. Research has been performed to develop methods to determine the association, size, and composition of ash-forming constituents in coal. Techniques are now available to determine the distribution of phases in fly ashes, deposits, and slags. Fundamental studies of the transformation of inorganic components to form intermediate ash components in the form of vapors, liquids, and solids have been performed using advanced analytical techniques.

Current conventional analytical methods for coal and coal ash materials do not provide adequate detail regarding their complex chemical and mineralogical properties. Advanced analytical techniques are currently being used to determine the association and forms of inorganic components in coals (7,8) and coal ash-derived materials (9,10). In addition, other laboratory-scale techniques are routinely used to determine viscosity, surface tension, sintering behavior, and deposit strength development (11,12). Utilization of these advanced analytical techniques, coupled with other laboratory methods, can potentially provide significant advances in understanding the behavior of inorganic components during combustion that will ultimately lead to better methods to predict and mitigate ash-related problems.

3.5.1 SEM Techniques

Automated scanning electron microscope/microprobe (SEM/EMPA) techniques are an effective means to examine coals, fly ashes, deposits, slags, soils, cements, and other complex heterogeneous materials. For example, these techniques provide the information needed to elucidate mechanisms of inorganic transformations which form intermediate ash, deposits, and slags during combustion and gasification. The SEM/EMPA system allows for observation and

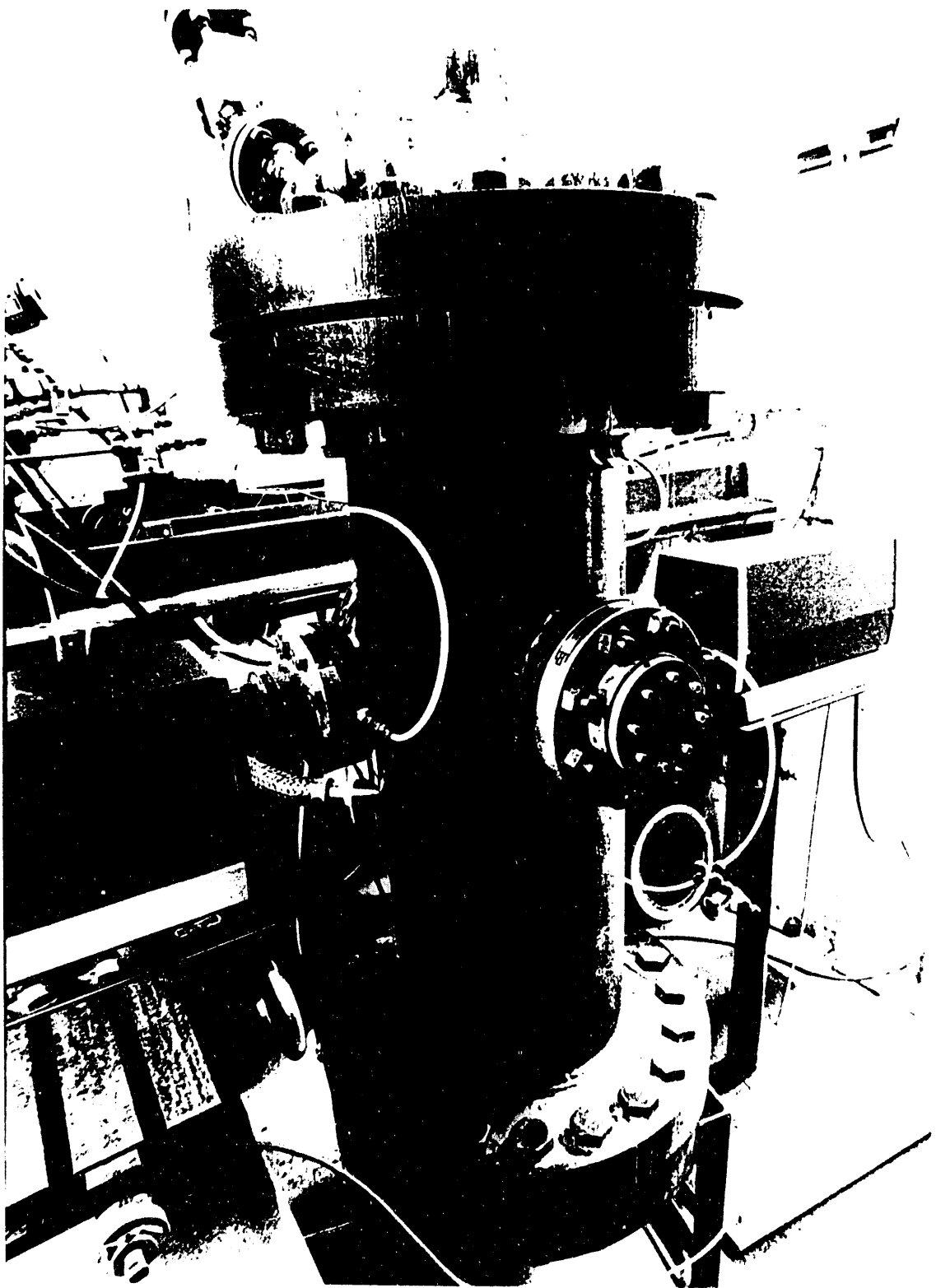


Figure 11. Photograph of pressurized spray chamber.

chemical analysis of very fine-grained phases while simultaneously preserving both the original chemistry of the minerals and their relationships to the organic constituents. Widespread applications of SEM/EMPA to coal include localized observation of the elemental content of macerals, determination of the morphology of organic maceral structures, identification of minerals, and description of the morphology of minerals. Automated SEM/EMPA and automated image analysis (AIA) techniques have been developed to quantify coal minerals. The automated SEM/EMPA techniques rely on the characterization of statistically significant numbers of particles to produce quantitative data on their size and chemistry.

Three SEM/EMPA techniques, computer-controlled scanning electron microscopy (CCSEM), scanning electron microscopy point count (SEMPC), and automated image analysis (AIA), are presently used in ash behavior in combustion and gasification systems research at the EERC. These techniques permit the study of transformations of inorganic constituents from the initial stages of coal conversion through the transformations that occur during ash deposition and slag formation. Their specific applications include 1) determination of the size, composition, and association of minerals in coals, 2) determination of the size and composition of intermediate ash components and fly ash, 3) determination of the degree of interaction (sintering) in ash deposits, and 4) identification and quantification of the components of ash deposits and slags--this includes liquid phase composition, reactivity, and crystallinity. By using SEM/EMPA for coals and throughout all stages of utilization, a continuity of data is achieved. The techniques which are routinely used by the Inorganic Analysis Research Lab (IARL) for examination of the inorganic components in coal and coal-derived materials are briefly described below.

CCSEM (7) is used to characterize unaltered coal samples and inorganic combustion products. A computer program is used to locate, size, and analyze particles. Because the analysis is automated, a large number of particles can be analyzed quickly and consistently. The heart of the CCSEM analysis system is a recently installed annular backscattered electron detector (BES). The BES system is used because the coefficient of backscatter (the fraction of the incoming beam that is backscattered) is proportional to the square root of the atomic number of the scattering atoms. This permits a high degree of resolution between sample components based on their atomic numbers. This means that coal minerals can be easily discerned from the coal matrix, and fly ash particles can be easily discerned from epoxy in polished sections. Brightness and contrast controls are used to optimize threshold levels between the coal matrix and mineral grains or fly ash particles. When a video signal falls between these threshold values, a particle is discerned and the particle center located. A set of eight rotated diameters about the center of the particle are measured, and the particle area, perimeter, and shape are calculated. The beam is then repositioned to the center of the particle, and an x-ray spectrum is obtained. The information is then stored to a Lotus transportable file for data reduction and manipulation. The CCSEM data provides quantitative information concerning not only the mineral types which are present, but their size and shape characteristics as well. Since the same analysis can be performed on the initial coal and resultant fly ash, direct comparisons can be made and inorganic transformations inferred.

The primary method used to characterize deposits is the scanning electron microscope/microprobe. The SEM is capable of imaging deposits and

determining the chemical composition of areas within deposits down to 1 micrometer in size. The use of the SEM is extremely valuable in identifying materials responsible for deposit initiation, growth, and strength development as well as the characterization of significant slag properties such as reactivity and viscosity. The SEM technique most often used to characterize entrained ashes and deposits is the SEMPC (8,9). This technique was developed to quantitatively determine the relative amount of phases present in ashes and deposits. The method involves microprobe analysis (chemical compositions) of a large number of random points in a polished cross section of a sample. In addition, x-ray diffraction is used to determine the crystalline phases present in the deposit as a support for the SEMPC analysis. Bulk chemical analysis of the deposit is also performed with x-ray fluorescence. This technique provides information on the degree of melting and interaction of the various deposited ash particles and provides quantitative information on the abundance of phases present in the ash. By examining the phases present, the material responsible for the formation of the deposit can be identified. In addition, various regions in deposits and individual entrained ash particles can be examined to determine the changes that occurred with time and, possibly, with changes in coal composition.

The CCSEM and SEMPC techniques are supplemented with morphological and chemical analysis of the microstructural features of the deposit. This is performed either by manually scanning across the sample, elemental mapping, or AIA. Automated digital imaging allows for the rapid, objective collection of digital images. Once the digital images have been collected and saved to disk, they can be manipulated in many constructive ways. Numerous applications for the digital images have been implemented at the EERC. Two methods using AIA to enhance the utility of the CCSEM and SEMPC techniques are described below.

The CCSEM technique described above is used for the standard analysis of coal. However, more detailed analysis of the coal minerals may be necessary. During pulverization of the coal, some coal minerals are liberated from the coal matrix. The mineral grains liberated from the matrix will experience different conditions and undergo different transformations and reactions than the minerals present within the coal matrix. Therefore, whether a mineral is contained within the coal matrix (included) or is separated from the coal matrix (excluded) is important when considering coal combustion. The term juxtaposition refers to mineral-to-mineral relationships and the relationship of minerals to the organic matrix of the coal.

The present method (7) used to determine the included/excluded and juxtaposition of the coal mineral matter involves the standard CCSEM analysis of the coal. However, prior to the analysis of each frame examined, a digital backscattered image is obtained and saved to the TN8500 image analysis system. As the CCSEM analysis proceeds each particle analyzed is identified on the image. The data can then be modified to include juxtapositional relationships.

The SEMPC technique does not provide all of the information needed to fully characterize a deposit or other material. It is also important to examine the morphology and physical relationships of the microscopic components of the deposit. While the SEMPC technique quantifies the chemistry and phase distributions, the morphologic characterization of deposits reveals the size, crystallinity, and juxtaposition of the phases present. The

morphologic investigation of the deposits provides insight into the sintering process as evidenced by the growth of necks between particles and the formation of a captive surface.

The major problem with morphologic information from the SEM is that it tends to be subjective, with the operator choosing areas of interest. A new technique (10) under development at the EERC will combine the SEMPC analysis with the morphologic investigation. The new analysis will collect quantitative chemical data from a grid pattern just as the present SEMPC program does; however, the new analysis will automatically collect digital images and save them to disk. The location of the points where EDS were collected will be plotted on the digital images. This will allow for detailed investigations of the positions of the phases identified by SEMPC. When combined with automated digital image analysis, this program will produce data detailing the chemistry, morphology, and juxtapositional nature of coal minerals and ash. These data will permit the quantification of parameters such as neck growth in deposits or thickness and composition of glassy phases in deposits and fly ash grains. The technique is currently being used to assess the characteristics of deposits produced in laboratory-, pilot-, and full-scale coal combustion systems. The SEMPC technique is combined with other methods of analysis to identify the compounds in the deposit that are causing the deposition problem. This information is used to trace the origin of the liquid phases back to the minerals and organically associated inorganic constituents in the original coal.

3.5.2 Sintering Behavior

Sintering is the process of consolidation of a solid substance of high surface area (for example, a powder) to a solid mass. In this process, the density of a given mass of sample will decrease compared to the initial sample. The sintering process is very important, because it is responsible, at least in part, for the formation of agglomerates, clinkers, and slags in coal combustion systems.

The sintering process requires mass transfer to occur. In the case of ash systems, the predominant mass transfer process is via viscous flow of liquid phase between adjacent particles. The relation of viscosity and surface tension to the sintering process has been discussed above. However, it is necessary to establish the rate at which the sintering occurs and the effect of viscosity and surface tension on the rate of sintering.

In sintering experiments, ash from a coal is produced under appropriate conditions to simulate various utilization environments. The density of the sintered masses will be determined using a pycnometer. Furthermore, the samples will be analyzed using x-ray diffraction, scanning electron microscopy, electron microprobe, and SEMPC. The detailed analysis will establish the various phases present and their relation to the sintering process. In particular, the SEMPC analysis will be used to establish the chemical composition of the component liquid phases responsible for sintering. The chemical composition will be used to predict the viscosity and surface tension of the component liquid phases.

3.5.3 XRF/XRD

The elemental content of bulk coal combustion products is determined by energy dispersive x-ray fluorescence spectrometry. Homogeneous finely ground sample powders are pressed into pellets and analyzed in a vacuum using a Kevex x-ray spectrometer equipped with a rhodium x-ray tube and six secondary targets. Interelement matrix effects are corrected for by using the EXACT (energy dispersive x-ray analysis computation technique) fundamental parameter routine. Calibration constants are derived from the analysis of certified standard reference materials and synthetic standards prepared from certified compounds. Analytical precision and accuracy are evaluated and optimized by analyzing at least one well-characterized coal ash standard during each analysis run. A new Kevex XRF system has been installed and will be in operation soon. The new system will increase our bulk chemical analysis abilities.

Qualitative x-ray powder diffraction is used to identify the crystalline phases present in coal combustion products. A representative aliquot of each sample powder is ground with ethyl alcohol and smeared onto a single-crystal, "zero"-background, quartz plate for subsequent analysis. Diffraction data are collected in 0.02° steps for a 1-second dwell time using a Phillips automated diffractometer equipped with a copper tube, theta-compensating slit, graphite-diffracted-beam monochromator, and scintillation detector. Software programs supplied by Materials Data Incorporated are used for data collection, data reduction, and phase identification.

3.5.4 The Chemical Fractionation Technique

The chemical fractionation procedure (11) is used to determine the modes of occurrence of inorganics present in coals. Chemical fractionation is especially valuable when the inorganics present in low-rank coals, which contain significant quantities of inorganics present as the salts of organic acid groups in the coal, are examined. CCSEM can determine the quantity of discrete minerals present in coals so, when combined with chemical fractionation, all of the inorganics present in coals can be determined.

The chemical fractionation procedure involves successive extractions with H_2O , 1 molar NH_4OAc , and 1 molar HCl . The elements that are extracted by H_2O are present in the coal as water-soluble compounds. Those that are extracted by NH_4OAc are present in an ion-exchangeable association (principally as the salts of carboxylic acids) that can be ion-exchanged for an ammonium ion from the solution, although gypsum ($CaSO_4 \cdot 2H_2O$) also dissolves during this extraction. HCl -extractable elements are present in the coal as acid-soluble minerals such as carbonates or sulfates, or in organic complexes with high coordination numbers.

3.5.5 Surface Science

Scanning Auger microscopy (SAM) is used for comprehensive surface analysis of a wide range of coal and coal-related materials. Capable of determining surface composition, chemical states, and depth profiling, the PHI 595 multiprobe instrument consists of three analytical systems: an Auger electron spectroscopy (AES) system capable of a 50×10^{-9} -meter-diameter electron beam, a cylindrical mirror electron analyzer, and a scanning system

and secondary electron detector to permit surface elemental mapping and high-resolution photographs. A 5-kV differentially pumped argon ion beam gun provides sputter-etching capability to acquire depth profile information. The x-ray photoelectron spectroscopy (XPS) system has a 10-kV Mg x-ray source and a beam diameter of about 2 mm. A double-pass, cylindrical mirror electron analyzer provides surface composition and chemical states. A secondary ion mass spectroscopy (SIMS) system utilizes the ion gun to ablate the sample surface to obtain trace element, isotopic, and molecular information. The positive and negative ions produced from the surface are analyzed by an energy-filtered quadrupole mass spectrometer.

3.6 Determination of Deposit Strengths

Deposits formed in the drop-tube furnace are removed from the coupon and measured for strength. The apparatus used to determine the crushing strength of ash deposits formed in the drop-tube furnace is shown in Figure 12. It consists of a miniature horizontal translator and a miniature pressure transducer. The translator (Ealing Electro Optics Model 37-0254) has a range of travel of 25 mm, a resolution of 0.1 μm , and a maximum translational speed of 15 mm/min. The pressure transducer (Precision Measurement Company Model 156) is a diaphragm strain gauge design with one active sensing face. The pressure range is 0-1000 psi. The transducer output is attached to a strain transducer indicator (Precision Measurement Company Model X). The transducer is mounted in a slot on top of an aluminum block and attached to the horizontal translator. A rod inserted in the side of the block meets the sensing face of the transducer and transmits the force exerted on the deposit as the translator moves.

4.0 RESULTS AND ACCOMPLISHMENTS

4.1 Fuel Preparation and Analyses

In order to learn about the potential for ash deposition on turbine blades, advanced analytical techniques were used to characterize raw Spring Creek coal and its beneficiated product to determine the abundance, size, and association of the inorganic constituents. The primary methods of analysis, in addition to conventional ASTM ashing followed by determination of the ash components, include chemical fractionation and computer-controlled scanning electron microscopy (CCSEM), used to determine the abundance of inorganic components associated both organically and inorganically in the coal. Chemical fractionation provides a means to determine the abundance of inorganic elements associated with the organic structure of the coal, while CCSEM is used to determine the size and composition of discrete mineral grains within the coal.

Tables 1 and 2 show the proximate, ultimate, and ash analyses of the three coals tested in the PDTF. The coals consisted of a raw Spring Creek coal; a Spring Creek coal which had been physically cleaned in a heavy media separator, acid-cleaned in a weak nitric acid leaching column and hot-water dried (HWD) and micronized; and a Spring Creek coal which had only been HWD and micronized (this fuel was supplied to Allison Gas Turbine Division for testing in their proof-of-concept coal-fired gas turbine). It can be seen from these analyses that the more deeply cleaned the coal, the lower the ash and sodium levels in the ash.

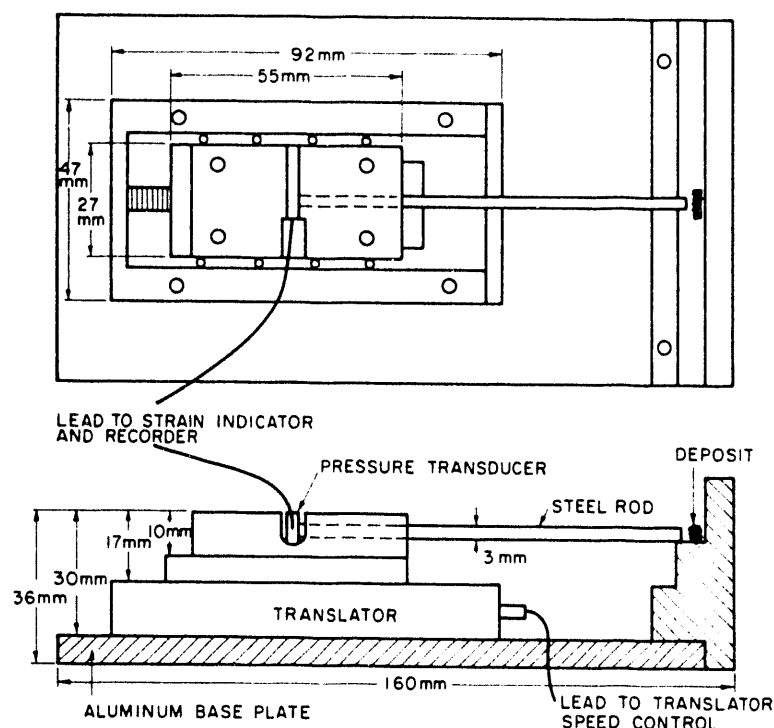


Figure 12. Deposit-strength measuring apparatus.

Chemical fractionation results for the Spring Creek coal are listed in Tables 3 and 4. These tables show the chemical fractionation results for the raw coal and the hydrothermally treated coal. Chemical fractionation was not performed on the acid-cleaned coal since little change in the amount of soluble cations was expected. For the raw coal, the solubility of the elements is very low, with the exception of phosphorus, calcium, sodium, potassium, and magnesium; this indicates that these elements are present primarily as the salts of organic acid groups, or as soluble minerals such as carbonates. The calcium was leached out with both ammonium acetate and HCl. The calcium removed by HCl may have been present as acid-soluble carbonate material, although CCSEM analysis indicates otherwise. The amount removed by ammonium acetate may reflect the presence of gypsum and organically bound calcium. A significant portion of the iron (16%) was also removed with ammonium acetate, indicating that some of the iron may be present in an ionic form. The remainder of the inorganic elements are present as discrete mineral grains, as indicated by their relative insolubility. The major differences between the raw coal and the CWF chemical fractionation results are consistent with the changes one would expect in inorganic content resulting from the treatment process. It appears that most of the salts of organic acid groups and soluble minerals are removed by the HWD process.

Tables 5 through 7 show the results of the CCSEM analysis on the PC/AC/HWD/micronized, the HWD/micronized, and the raw coals. The CCSEM analysis of the PC/AC/HWD/micronized Spring Creek fuel indicates that the fuel is concentrated in quartz, aluminosilicates, pyrite, and iron oxide, although

TABLE 1

Proximate and Ultimate Analyses of Fuels Tested

| Sample: | Raw Spring Creek Coal | HWD Spring Creek | PC/AC/HWD Spring Creek |
|------------------------------------|--------------------------|---------------------|---------------------------|
| PDU Test No. | NA | 55 | 45 |
| Prox. Anal. (mf) | | | |
| Volatile Matter | 43.48 | 42.82 | 39.62 |
| Fixed Carbon | 51.70 | 52.58 | 56.21 |
| Ash | 4.82 | 4.60 | 2.07 |
| Ult. Anal. (mf) | | | |
| Hydrogen | 4.75 | 4.66 | 4.51 |
| Carbon | 72.52 | 73.22 | 75.00 |
| Nitrogen | 0.86 | 0.97 | 1.37 |
| Sulfur | 0.41 | 0.40 | 0.35 |
| Oxygen (diff.) | 16.94 | 16.12 | 16.70 |
| Ash | 4.82 | 4.60 | 2.07 |
| Heating Value (mf, Btu/lb) | 12,260 | 12,693 | 12,820 |
| Ash Fusion Temp. Deg F-Reducing | | | |
| Init. Deform. | ND | ND | 2,148 |
| Softening | ND | ND | 2,278 |
| Hemispherical | ND | ND | 2,310 |
| Fluid | ND | ND | 2,313 |
| Part. Size-Mean (microns) | 54 | 13 | 15 |
| Top Size (99%<) (microns) | 348 | 100 | 81 |

TABLE 2

X-Ray Fluorescence Analysis of LRC Fuels Tested in Turbine Program:
High-Temperature Ash Results (% of ash, SO₃-free)

| Sample: | Raw Spring Creek Coal | HWD Spring Creek | PC/AC/HWD Spring Creek |
|--------------------------------|--------------------------|---------------------|---------------------------|
| PDU Test No. | NA | 55 | 45 |
| SiO ₂ | 29.2 | 31.0 | 33.5 |
| Al ₂ O ₃ | 18.7 | 21.3 | 31.9 |
| Fe ₂ O ₃ | 8.1 | 9.6 | 14.7 |
| TiO ₂ | 2.3 | 2.0 | 3.3 |
| P ₂ O ₅ | 1.2 | 0.6 | 0.9 |
| CaO | 23.0 | 22.0 | 10.1 |
| MgO | 7.6 | 7.8 | 4.3 |
| Na ₂ O | 9.0 | 5.5 | 1.0 |
| K ₂ O | 0.8 | 0.2 | 0.2 |
| Total | 99.9 | 100.0 | 99.9 |

TABLE 3

Chemical Fractionation Results of Raw Spring Creek Coal (wt%)

| | Initial (ppm) | Removed by H ₂ O | Removed by NH ₄ OAc | Removed by HCl | Remaining |
|------------|------------------|--------------------------------|-----------------------------------|-------------------|-----------|
| Silicon | 4273 | 0 | 0 | 0 | 100 |
| Aluminum | 3997 | 3 | 6 | 49 | 42 |
| Iron | 2442 | 0 | 16 | 72 | 12 |
| Titanium | 604 | 0 | 45 | 0 | 55 |
| Phosphorus | 315 | 2 | 73 | 22 | 3 |
| Calcium | 6688 | 0 | 59 | 40 | 0 |
| Magnesium | 2024 | 1 | 79 | 17 | 2 |
| Sodium | 3058 | 34 | 65 | 1 | 1 |
| Potassium | 790 | 65 | 25 | 2 | 8 |

* Results are expressed with silicon loss normalized to zero.

TABLE 4

Chemical Fractionation Results of Hydrothermally Treated
Spring Creek Coal (wt%)

| | Initial (ppm) | Removed by H ₂ O | Removed by NH ₄ OAc | Removed by HCl | Remaining |
|------------|------------------|--------------------------------|-----------------------------------|-------------------|-----------|
| Silicon | 7702 | 0 | 0 | 0 | 100 |
| Aluminum | 4634 | 0 | 0 | 0 | 100 |
| Iron | 2712 | 6 | 4 | 45 | 44 |
| Titanium | 427 | 0 | 3 | 0 | 97 |
| Phosphorus | 108 | 0 | 12 | 64 | 24 |
| Calcium | 6902 | 0 | 30 | 55 | 15 |
| Magnesium | 2725 | 0 | 42 | 51 | 7 |
| Sodium | 489 | 6 | 82 | 3 | 9 |
| Potassium | 161 | 0 | 20 | 0 | 80 |

* Results are expressed with silicon loss normalized to zero.

the high iron oxide levels could also be due to contamination from the magnetite heavy media used in the physical cleaning process. CCSEM analysis of the Allison fuel and the raw coal shows that the dominant minerals present are quartz and kaolinite, with significant amounts of other aluminosilicates, including montmorillonite, and potassium aluminosilicate. The presence of a significant amount of pyrite was also noted. The results indicate that the hot-water-drying process slightly reduced the total amounts of inorganic constituents present; however, the relative amounts of discrete minerals remained constant. The CCSEM size analysis indicates that the micronized coals were dominated by minerals in the 2.2- to 10.0-micrometer size range while the size distribution of minerals in the raw coal was much more

TABLE 5

Summary of CCSEM Results for PC/AC/HWD Spring Creek Fuel

| Particle-Size Distribution, μm : Wt% Mineral Basis | <2.2 | 2.2- 4.6 | 4.6- 10.0 | 10.0- 22.0 | 22.0- 46.0 | >46.0 | Total |
|---|-------------|-------------|--------------|---------------|---------------|------------|--------------|
| Quartz | 15.7 | 14.9 | 0.6 | 0.0 | 0.0 | 0.0 | 31.1 |
| Iron Oxide | 3.6 | 5.5 | 0.0 | 0.0 | 0.0 | 0.0 | 9.1 |
| Aluminosilicate | 26.9 | 11.5 | 1.1 | 0.0 | 0.0 | 0.0 | 39.5 |
| Ca Al-Silicate | 0.0 | 0.2 | 0.0 | 0.0 | 0.0 | 0.0 | 0.2 |
| Fe Al-Silicate | 0.2 | 0.0 | 0.0 | 0.0 | 0.0 | 0.0 | 0.2 |
| K Al-Silicate | 1.0 | 0.2 | 0.0 | 0.0 | 0.0 | 0.0 | 1.2 |
| Pyrite | 7.7 | 1.4 | 0.0 | 0.0 | 0.0 | 0.0 | 9.1 |
| Barite | 0.0 | 0.2 | 0.0 | 0.0 | 0.0 | 0.0 | 0.2 |
| Gyp/Al-Silicate | 0.1 | 0.0 | 0.0 | 0.0 | 0.0 | 0.0 | 0.1 |
| Ca Aluminate | 0.2 | 0.1 | 0.0 | 0.0 | 0.0 | 0.0 | 0.3 |
| Spinel | 0.1 | 0.0 | 0.0 | 0.0 | 0.0 | 0.0 | 0.1 |
| Rutile | 0.4 | 1.1 | 0.0 | 0.0 | 0.0 | 0.0 | 1.5 |
| Pyrrhotite/Sulfate | 0.4 | 0.0 | 0.0 | 0.0 | 0.0 | 0.0 | 0.4 |
| Si-rich | 0.5 | 2.4 | 0.0 | 0.0 | 0.0 | 0.0 | 2.9 |
| Unknown | 1.7 | 2.0 | 0.6 | 0.0 | 0.0 | 0.0 | 4.3 |
| Total | 58.3 | 39.5 | 2.2 | 0.0 | 0.0 | 0.0 | 100.0 |

dispersed. Obviously, the processing preferentially removes some of the larger minerals and reduces the size of the remaining minerals. This is an important factor when considering ash behavior because it affects both ash particle chemistry and aerodynamic behavior in the utilization system.

Tables 8 and 9 show the CCSEM analysis with image analysis for determining juxtaposition of the mineral particles for both the Allison HWD/micronized and raw Spring Creek fuels. These tables indicate that the cleaned coals tend to contain more inherent coal particles presumably because the physical cleaning and centrifugation processes would separate the finer mineral particles.

4.2 Coal-Water Fuel Atomization

Due to manpower and equipment constraints, very limited CWF atomization testing was completed during the reporting period.

Spray testing of Spring Creek CWF was conducted during the reporting period using a new Delavan external mix atomizer. These atomization tests were conducted to obtain high speed photographs using this new atomizer. Results from these atomization tests indicate that the atomizer had a lower pressure ratio at comparable atomizing air-to-fuel ratios than the Delavan external mix atomizer. These photographs indicated that at the lower atomizing air-to-fuel ratios (< 1.25) the spray pattern was becoming much less dispersed. It was apparent that this atomizer was significantly oversized for the flowrates utilized in these tests and did not provide very meaningful information.

TABLE 6

Summary of CCSEM Results for HWD/Micronized Spring Creek Fuel
Produced for Allison Gas Turbines

| Particle-Size Distribution, μm : Wt% Mineral Basis | <2.2 | 2.2- 4.6 | 4.6- 10.0 | 10.0- 22.0 | 22.0- 46.0 | >46.0 | Total |
|---|------|-------------|--------------|---------------|---------------|-------|-------|
| Quartz | 15.0 | 7.9 | 1.3 | 0.8 | 0.5 | 0.0 | 25.5 |
| Iron Oxide | 2.1 | 2.2 | 0.0 | 0.0 | 0.0 | 0.0 | 4.4 |
| Rutile | 0.9 | 0.7 | 0.0 | 0.0 | 0.0 | 0.0 | 1.7 |
| Alumina | 0.3 | 0.0 | 0.0 | 0.0 | 0.0 | 0.0 | 0.3 |
| Calcite | 0.3 | 0.3 | 0.0 | 0.0 | 0.0 | 0.0 | 0.6 |
| Dolomite | 0.0 | 0.0 | 0.7 | 0.0 | 0.0 | 0.0 | 0.7 |
| Kaolinite | 11.2 | 8.2 | 2.8 | 0.2 | 0.0 | 0.0 | 22.4 |
| Montmorillonite | 5.5 | 2.2 | 0.0 | 0.0 | 0.0 | 0.0 | 7.7 |
| K Al-Silicate | 1.0 | 0.6 | 0.0 | 0.0 | 0.0 | 0.0 | 1.6 |
| Fe Al-Silicate | 0.3 | 0.2 | 0.0 | 0.0 | 0.0 | 0.0 | 0.5 |
| Ca Al-Silicate | 1.1 | 0.7 | 0.0 | 0.1 | 0.0 | 0.0 | 1.7 |
| Aluminosilicate | 0.1 | 0.0 | 0.0 | 0.0 | 0.0 | 0.0 | 0.1 |
| Mixed Al-Silicate | 0.6 | 0.0 | 0.0 | 0.0 | 0.0 | 0.0 | 0.6 |
| Fe Silicate | 0.0 | 0.8 | 0.0 | 0.0 | 0.0 | 0.0 | 0.8 |
| Ca Silicate | 0.1 | 0.2 | 0.0 | 0.0 | 0.0 | 0.0 | 0.4 |
| Pyrite | 4.7 | 0.6 | 0.0 | 0.0 | 0.0 | 0.0 | 5.3 |
| Pyrrhotite | 0.1 | 0.0 | 0.0 | 0.0 | 0.0 | 0.0 | 0.1 |
| Oxidized Pyrrhotite | 0.9 | 0.9 | 0.0 | 0.3 | 0.0 | 0.0 | 2.0 |
| Gypsum | 0.2 | 0.0 | 0.0 | 0.0 | 0.0 | 0.0 | 0.2 |
| Barite | 1.8 | 1.1 | 0.0 | 0.0 | 0.0 | 0.0 | 3.0 |
| Apatite | 0.0 | 0.2 | 0.0 | 0.0 | 0.0 | 0.0 | 0.2 |
| Ca Al-P | 0.5 | 1.2 | 0.0 | 0.0 | 0.0 | 0.0 | 1.7 |
| Gypsum/Barite | 0.8 | 0.0 | 0.0 | 0.0 | 0.0 | 0.0 | 0.8 |
| Gyp/Al-Silicate | 0.5 | 0.2 | 0.0 | 0.3 | 0.0 | 0.0 | 0.9 |
| Si-Rich | 0.5 | 0.8 | 0.0 | 0.4 | 0.7 | 0.0 | 2.3 |
| Ca-Rich | 0.2 | 0.0 | 0.0 | 0.0 | 0.0 | 0.0 | 0.2 |
| Ca-Si Rich | 0.1 | 0.0 | 0.0 | 0.0 | 0.0 | 4.5 | 4.6 |
| Unknown | 5.4 | 0.6 | 0.9 | 1.8 | 1.1 | 0.0 | 9.8 |
| Total | 54.0 | 29.8 | 5.6 | 3.8 | 2.3 | 4.5 | 100.0 |

Atomization tests utilizing a Spring Creek CWF and the Delavan Swirl-Air nozzle employed in previous combustion testing were also attempted during the reporting period. Observation of the spray cone indicated that at the lower atomizing air-to-fuel ratios the spray would become flat. The atomizing air-to-fuel ratio at which the spray would become flat increased with increasing spray chamber pressure. The reason for this nozzle behavior is not understood at this time, but it is felt that this phenomenon did not occur during the combustion tests performed in 1-MM Btu/hr gas turbine simulator using this same atomizer.

4.3 PDTF Combustion Testing With Beneficiated Fuels

Pressurized drop-tube furnace (PDTF) testing was conducted using the fuels described above. A series of shakedown tests was conducted to measure

TABLE 7

Summary of CCSEM Results for Raw Spring Creek Fuel (-325 mesh)

| Particle-Size Distribution, μm : Wt% Mineral Basis | <2.2 | 2.2- 4.6 | 4.6- 10.0 | 10.0- 22.0 | 22.0- 46.0 | >46.0 | Total |
|---|------|-------------|--------------|---------------|---------------|-------|-------|
| Quartz | 4.0 | 5.3 | 4.5 | 4.6 | 4.1 | 0.0 | 22.4 |
| Iron Oxide | 0.2 | 0.1 | 1.0 | 0.7 | 0.4 | 2.5 | 4.9 |
| Rutile | 0.2 | 0.0 | 0.3 | 0.1 | 0.0 | 0.0 | 0.7 |
| Calcite | 0.3 | 0.3 | 0.0 | 0.0 | 0.0 | 0.0 | 0.6 |
| Kaolinite | 1.9 | 2.8 | 4.7 | 4.9 | 5.6 | 2.4 | 22.3 |
| Montmorillonite | 0.5 | 1.1 | 0.9 | 0.5 | 1.2 | 0.0 | 4.1 |
| K Al-Silicate | 1.0 | 2.0 | 1.8 | 1.0 | 1.1 | 0.0 | 6.9 |
| Fe Al-Silicate | 0.2 | 0.0 | 0.0 | 0.1 | 0.0 | 0.0 | 0.2 |
| Ca Al-Silicate | 0.1 | 0.0 | 0.0 | 0.0 | 0.0 | 0.0 | 0.1 |
| Aluminosilicate | 0.2 | 0.6 | 1.1 | 0.1 | 0.0 | 0.0 | 2.0 |
| Mixed Al-Silicate | 0.1 | 0.2 | 0.0 | 0.0 | 0.2 | 0.0 | 0.4 |
| Pyrite | 1.1 | 0.4 | 0.9 | 1.1 | 2.5 | 1.1 | 7.2 |
| Pyrrhotite | 0.2 | 0.0 | 0.0 | 0.1 | 0.6 | 0.0 | 0.8 |
| Oxidized Pyrrhotite | 0.0 | 0.3 | 0.0 | 0.0 | 0.0 | 0.0 | 0.4 |
| Gypsum | 0.3 | 1.2 | 0.0 | 0.1 | 0.2 | 0.0 | 1.8 |
| Barite | 0.7 | 0.5 | 0.9 | 0.3 | 0.7 | 0.0 | 3.1 |
| Ca Al-P | 0.1 | 0.4 | 0.0 | 0.2 | 0.0 | 0.0 | 0.7 |
| Gypsum/Barite | 0.1 | 0.0 | 0.0 | 0.0 | 0.0 | 0.0 | 0.1 |
| Gyp/Al-Silicate | 0.2 | 0.0 | 0.0 | 0.4 | 0.0 | 1.0 | 1.6 |
| Si-Rich | 0.5 | 0.9 | 1.0 | 0.8 | 1.6 | 2.4 | 7.1 |
| Ca-Rich | 0.1 | 0.2 | 0.0 | 0.0 | 0.0 | 0.0 | 0.3 |
| Unknown | 1.6 | 1.4 | 0.9 | 3.3 | 4.8 | 0.0 | 12.0 |
| Total | 13.7 | 17.6 | 18.0 | 18.4 | 22.8 | 9.4 | 100.0 |

the carbon burnout achieved using the Allison fuel (HWD/micronized) Spring Creek (AFSPC). After optimization of the burnout tests, other fly ash collection tests were conducted using the physically cleaned, acid-cleaned, HWD/micronized Spring Creek (APSPC) and the raw Spring Creek (SPCRK) fuels. Tables 10 through 14 show the operating conditions, weights of fly ash collected, and the measured burnouts for these combustion tests. Percent ash in the fly ash was measured using a modified TGA technique since sample sizes were too small to perform ASTM loss-on-ignition (LOI) tests. Carbon burnout was calculated using the equation given below by Wenglarz and others (13):

$$\text{Carbon burnout fraction} = (1 - W_a/W_x)/(1 - W_a)$$

where W_x is the weight fraction of ash in the particulate sample and W_a is the weight fraction of ash in the coal from which the slurry was made.

Initial combustion tests were performed using a bulk filter to capture all of the fly ash. Starting with Test Number 37, the number 2 and 5 cyclones of a multicyclone set along with a final filter were used to collect size-fractionated fly ash samples. The three fractions were then submitted for analysis by SEM point count, particle size using the small sample cell on a Malvern 2600, and LOI tests using the modified TGA technique if enough sample

TABLE 8

CCSEM Analysis with Image Analysis for Allison HWD/Micronized
Spring Creek Fuel

| Mineral Types | Number | Frequency | % Extraneous | % Inherent |
|------------------------|--------|-----------|--------------|------------|
| Quartz | 22 | 20.56 | 23 | 77 |
| Montmorillonite | 5 | 4.67 | 20 | 80 |
| K-Aluminosilicate | 2 | 1.87 | 0 | 100 |
| Kaolinite | 15 | 14.02 | 27 | 73 |
| Ca-Aluminosilicate | 1 | 0.93 | 0 | 100 |
| Ca-Silicate | 1 | 0.93 | 0 | 100 |
| Oxidized Pyrrhotite | 2 | 1.87 | 50 | 50 |
| Pyrite | 6 | 5.61 | 17 | 83 |
| Gypsum | 1 | 0.93 | 0 | 100 |
| Mixed Silicates | 1 | 0.93 | 0 | 100 |
| Gypsum/Aluminosilicate | 3 | 2.80 | 33 | 67 |
| Si-Rich | 5 | 4.67 | 40 | 60 |
| Ca-Si-Rich | 1 | 0.93 | 0 | 100 |
| Fe-Al-Silicate | 1 | 0.93 | 0 | 100 |
| Unknown | 41 | 38.32 | 7 | 93 |
| Total | 107 | 100.0 | | |

remained. Entrained alkali gettering tests (SPCRK 42 and 43) were performed by adding kaolin to the raw Spring Creek at a level that would increase the ash content by approximately 50 percent.

Tables 15 through 20 show the scanning electron microprobe point count (SEMPC) and particle-size analyses of the fly ash samples from samples analyzed to this point. Other analyses will be performed at a later date as analytical time on the SEM becomes available. Analyses of the raw Spring Creek fly ash indicate that the final filter is high in sodium sulfates and sodium calcium sulfates, which would be expected to cause severe alkali deposition and corrosion problems in a coal-fired gas turbine. Addition of the kaolin to the raw Spring Creek appeared to affect the distribution of the sodium species reducing the amount of sodium species found in the smallest size range (i.e., final filter). Figures 13 and 14 show the weight percent of the total elements as collected in each size fraction. As can be seen the addition of the kaolin reduced the percent of Na_2O collected in the final filter by a factor of two. Operating pressure did not seem to affect this shift in where the sodium species are collected. The cut points of the multicyclones were significantly different under atmospheric pressure such that a direct comparison cannot be made.

A comparison of the fly ash composition and particle-size distribution is also given in these tables. Both the PC/AC/HWD/micronized and the Allison HWD/micronized Spring Creek fuels had lower sodium levels in the final filter fraction than the raw Spring Creek fuel. This is expected since acid-cleaning and hot-water-drying processes have been shown to reduce the sodium levels of the coal ash. However, it also appears that the HWD/micronized Spring Creek fuel has lower sodium levels than the more deeply cleaned Spring Creek fuel, which is not expected. One possible explanation is that the CCSEM analyses

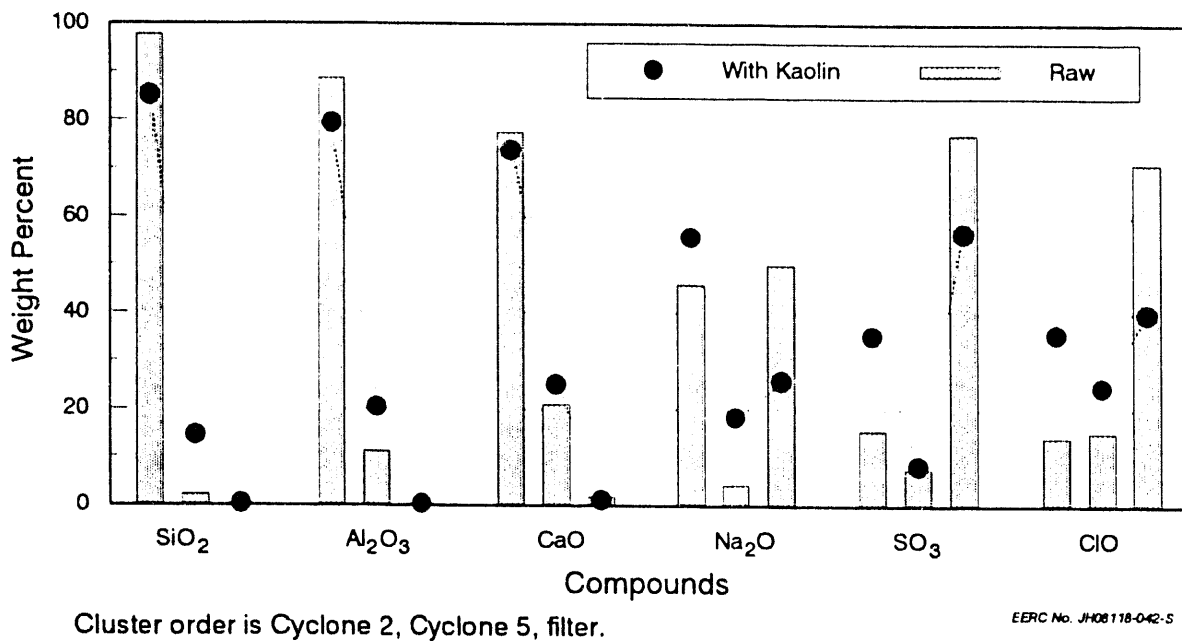


Figure 13. Weight percent of total elements in each size fraction for Spring Creek coal combustion testing at 100 psi with and without Kaolin addition.

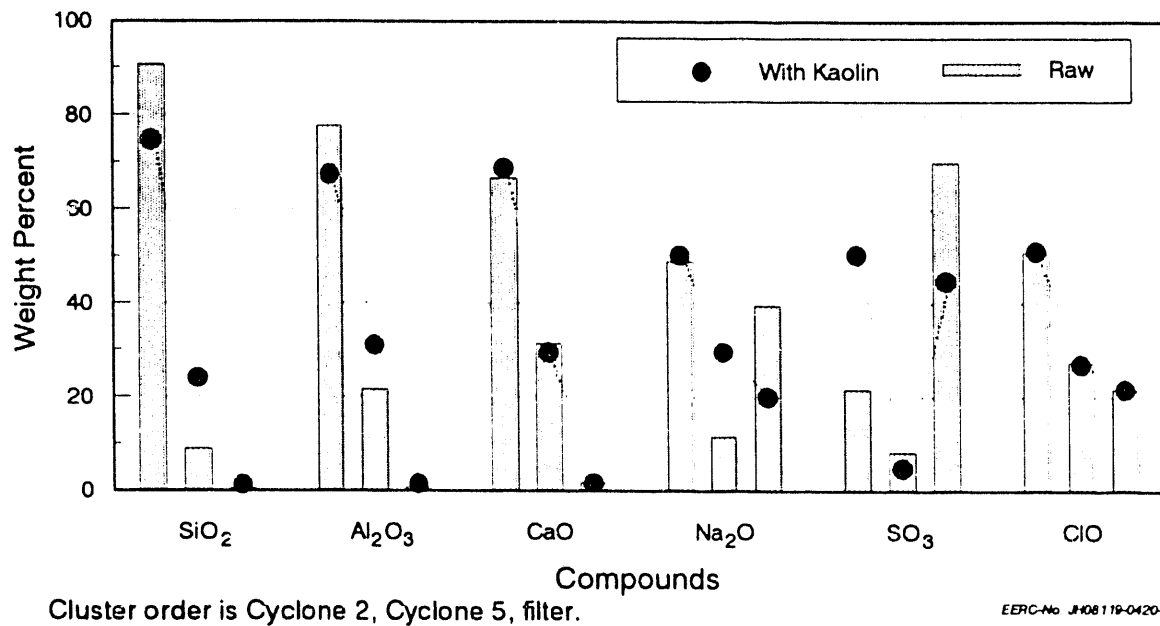


Figure 14. Weight percent of total elements in each size fraction for Spring Creek Coal combustion testing at atmospheric pressure with and without kaolin addition.

TABLE 9

| CCSEM Analysis with Image Analysis for Raw Spring Creek Fuel | | | | |
|--|--------|-----------|--------------|------------|
| Mineral Types | Number | Frequency | % Extraneous | % Inherent |
| Quartz | 102 | 24.46 | 39 | 61 |
| Montmorillonite | 10 | 2.40 | 60 | 40 |
| K-Aluminosilicate | 23 | 5.52 | 61 | 39 |
| Kaolinite | 90 | 21.58 | 58 | 42 |
| Iron Oxide | 5 | 1.20 | 60 | 40 |
| Ca-Aluminosilicate | 2 | 0.48 | 50 | 50 |
| Na-Aluminosilicate | 1 | 0.24 | 0 | 100 |
| Rutile | 3 | 0.72 | 0 | 100 |
| Pyrrhotite | 3 | 0.72 | 33 | 67 |
| Oxidized Pyrrhotite | 1 | 0.24 | 100 | 0 |
| Pyrite | 13 | 3.12 | 54 | 46 |
| Gypsum | 9 | 2.16 | 67 | 33 |
| Barite | 12 | 2.88 | 58 | 42 |
| Calcite | 5 | 1.20 | 80 | 20 |
| Ca-Al-Phosphate | 3 | 0.72 | 33 | 67 |
| Mixed Silicates | 1 | 0.24 | 0 | 100 |
| Aluminosilicate | 3 | 0.72 | 33 | 67 |
| Gypsum/Barite | 1 | 0.24 | 0 | 100 |
| Gypsum/Aluminosilicate | 7 | 1.68 | 29 | 71 |
| Si-Rich | 22 | 5.28 | 59 | 41 |
| Ca-Rich | 4 | 0.96 | 0 | 100 |
| Fe-Al-Silicate | 2 | 0.48 | 50 | 50 |
| Unknown | 95 | 22.78 | 26 | 74 |
| Total | 417 | 100.00 | | |

indicate that a significant quantity of kaolinite appears in the small size ranges of the Allison fuel, while there appears to be no kaolinite in the deeply cleaned fuel. The deep cleaning appears to remove some inorganic components which might be acting as effective alkali getters, thus accounting for the sodium concentration increase in the more deeply cleaned fuel.

Particle-size analyses of these fractions as determined by the small sample cell on the Malvern 2600 indicate that the final filter tended to have the largest particle-size distribution among the three collection devices (i.e., the #2 and #5 cyclones and the final filter) which is physically impossible given the operating principles of a multicyclone sampling system. Further examination of the final filter samples was conducted by SEM. Figures 15 and 16 are high-magnification photographs of filter cake from a final filter sample. These photographs indicate that the filter cake consists of very fine (< 1 μm) particles which have agglomerated into larger flakes. It is believed that the Malvern particle-size distribution actually is measuring the size of the agglomerated flakes.

The PDTF testing has also been directed to perform tests for a separate multiclient contract concerning coal ash behavior under reducing environments. No PDTF testing under this project was completed during the last two months of the reporting period.

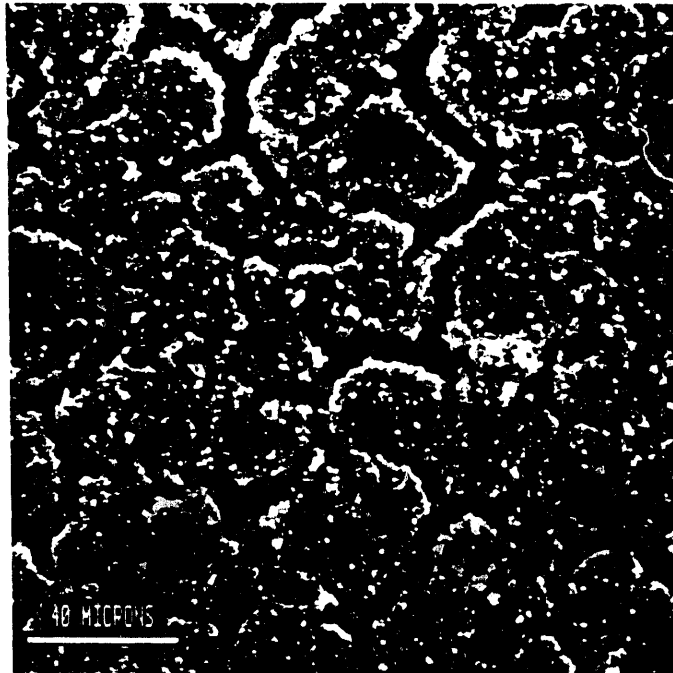


Figure 15. Photograph of flakes of final filter cake.

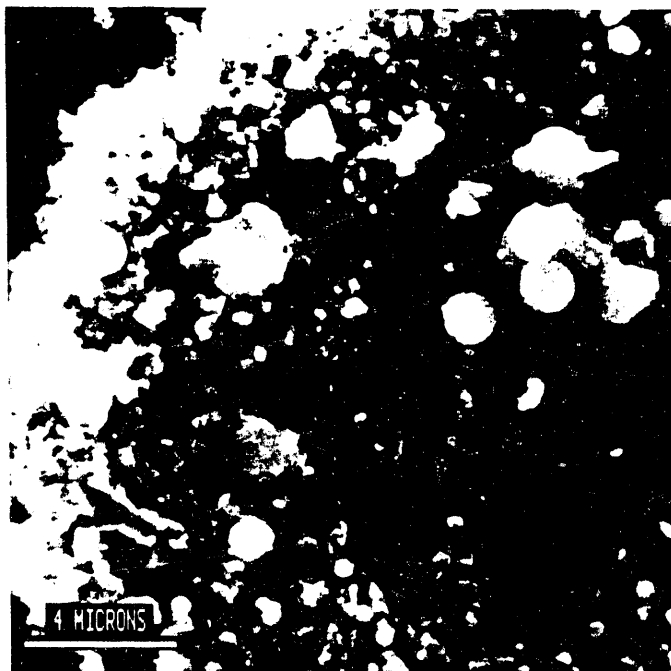


Figure 16. High-magnification photograph of final filter cake.

TABLE 10

Operating Conditions and Results from Shakedown Combustion Tests Using Allison Fuel Spring Creek Coal

| | AFSPC01 | AFSPC02 | AFSPC03 | AFSPC04 | AFSPC05 | AFSPC07 | AFSPC08 | AFSPC09 | AFSPC10 | AFSPC11 | AFSPC14 |
|--------------------------------------|---------|---------|---------|---------|---------|---------|---------|---------|---------|---------|---------|
| Coal Feed Rate (g/min) | 0.1530 | 0.1209 | 0.0679 | 0.3376 | 0.1405 | 0.3955 | 0.1134 | 0.4213 | 0.2454 | 0.4485 | 0.3913 |
| Total Weight Coal Fed (g) | 2.3 | 4.3 | 1.7 | 6.6 | 6.2 | 11.7 | 3.7 | 9.5 | 6.4 | 9.0 | 10.2 |
| Weight Ash Collected (g) | 0.0917 | 0.6923 | 0.2000 | 0.3247 | 0.1726 | 0.4123 | 0.1837 | 0.2869 | 0.2602 | 0.2188 | .1545 |
| Weight Ash Feed (g) | 0.1058 | 0.1978 | 0.0782 | 0.3036 | 0.2852 | 0.5382 | 0.1702 | 0.4370 | 0.2944 | 0.4140 | 0.4504 |
| Percent Ash in Fly Ash (mf) | 47.4 | 5.44 | 10.97 | 12.86 | 13.05 | 19.64 | 8.19 | 12.73 | 15.33 | 26.41 | 69.88 |
| Fly Ash Carbon Burnout (%) | 94.65 | 16.19 | 60.87 | 67.33 | 67.87 | 80.27 | 45.95 | 66.94 | 73.37 | 86.56 | 97.92 |
| Feeder Air Flow Rate (slpm) | 20.0 | 20.0 | 8.0 | 10.0 | 11.2 | 10.0 | 10.0 | 10.0 | 10.0 | 10.0 | 8.0 |
| Avg. Air Flow Rate (slpm) | 99.9 | 99.9 | 15.0 | 39.9 | 39.9 | 39.9 | 39.9 | 39.9 | 89.9 | 39.7 | 5.0 |
| Avg. N ₂ Flow Rate (slpm) | 99.9 | 99.9 | 15.0 | 50.0 | 50.0 | 49.9 | 49.9 | 49.9 | 89.7 | 49.9 | 13.0 |
| Initial Oxygen Conc. (mol%) | 11.5 | 11.5 | 12.7 | 10.5 | 10.6 | 10.5 | 10.5 | 10.5 | 11.0 | 10.5 | 10.5 |
| % Excess Air | 10,746 | 13,624 | 4,592 | 1,945 | 4,937 | 1,646 | 5,988 | 1,540 | 5,535 | 1,433 | 195 |
| Exit Gas Equivalence Ratio | 0.0092 | 0.0073 | 0.0213 | 0.0489 | 0.0199 | 0.0573 | 0.0164 | 0.0610 | 0.0177 | 0.0652 | 0.3393 |
| PDTF Pressure (psig) | 133.3 | 133.3 | 3.1 | 5.6 | 5.4 | 5.4 | 5.1 | 4.9 | 19.2 | 7.2 | 1.1 |
| Zone 1 Tube Temp. (°C) | 1,197 | 1,128 | 1,248 | 1,198 | 1,398 | 1,398 | 1,398 | 1,398 | 1,251 | 1,395 | 1,267 |
| Zone 2 Tube Temp. (°C) | 1,248 | 1,247 | 1,248 | 1,198 | 1,398 | 1,398 | 1,398 | 1,398 | 1,370 | 1,398 | 1,298 |
| Zone 3 Tube Temp. (°C) | 1,245 | 1,245 | 1,245 | 1,195 | 1,218 | 1,229 | 1,396 | 1,229 | 1,226 | 1,225 | 1,296 |
| Optical Zone Temp. (°C) | 798 | 773 | 952 | 872 | 907 | 899 | 972 | 792 | 882 | 910 | 1,055 |
| Zone 4 Tube Temp. (°C) | 815 | 800 | 1,247 | 1,197 | 1,197 | 1,197 | 1,342 | 998 | 1197 | 1197 | 1,283 |
| Substrate Metal Temp. (°C) | 199 | 188 | 67 | 148 | 154 | 169 | 188 | 169 | 160 | 176 | 40 |
| Prim. Gas Vel. (m/s) | 2.03 | 2.03 | 6.75 | 7.37 | 8.39 | 7.48 | 7.56 | 7.69 | 4.45 | 6.91 | 7.71 |
| Total Gas Vel. (m/s) | 0.41 | 0.41 | 0.59 | 1.32 | 1.37 | 1.36 | 1.54 | 1.40 | 1.53 | 1.25 | 0.47 |
| Accelerator Gas Vel. (m/s) | 14.8 | 59.3 | 21.4 | 47.5 | 49.4 | 49.1 | 55.4 | 50.3 | 55.2 | 45.0 | 17.0 |
| Avg. Residence Time (s) | 0.97 | 0.97 | 0.93 | 0.47 | 0.45 | 0.46 | 0.40 | 0.45 | 0.41 | 0.50 | 0.85 |

TABLE 11

Operating Conditions and Results from Shakedown Combustion Tests Using Allison Fuel Spring Creek Coal

| | AFSPC15 | AFSPC16 | AFSPC17 | AFSPC18 | AFSPC19 | AFSPC20 | AFSPC21 | AFSPC22 | AFSPC23 | AFSPC24 | AFSPC25 |
|--------------------------------------|---------|---------|---------|---------|---------|---------|---------|---------|---------|---------|---------|
| Coal Feed Rate (g/min) | 0.3875 | 0.6028 | 0.3737 | 0.4163 | 0.2052 | 0.2145 | 0.3984 | 0.2657 | 0.4136 | 0.1833 | 0.4915 |
| Total Weight Coal Fed (g) | 10.1 | 13.0 | 9.0 | 12.8 | 6.1 | 4.0 | 7.0 | 6.4 | 8.5 | 9.5 | 10.6 |
| Weight Ash Collected (g) | 0.0926 | 0.3228 | 0.1244 | 0.6184 | 0.7023 | 0.3912 | 0.0330 | 1.7668 | 0.1056 | 0.2478 | 3.3245 |
| Weight Ash Feed (g) | 0.446 | 0.574 | 0.397 | 0.565 | 0.269 | 0.177 | 0.309 | 0.283 | 0.375 | 0.420 | 0.468 |
| Percent Ash in Fly Ash (mf) | 48.99 | 75.42 | ND | 31.56 | 18.25 | 17.77 | 4.6 | 10.9 | 56.15 | 89.39 | 6.52 |
| Fly Ash Carbon Burnout (%) | 95.0 | 98.4 | ND | 89.5 | 78.4 | 77.7 | 0 | 60.6 | 96.2 | 99.4 | 30.9 |
| Avg. Feeder Air Flow Rate (slpm) | 10.0 | 10.0 | 20.0 | 20.0 | 20.0 | 20.0 | 20.0 | 20.0 | 8.0 | 10.0 | 10.0 |
| Avg. Sec. Air Flow Rate (slpm) | 30.0 | 90.0 | 99.9 | 99.9 | 99.9 | 99.9 | 20.0 | 20.0 | 5.0 | 30.0 | 89.7 |
| Avg. N ₂ Flow Rate (slpm) | 39.9 | 99.9 | 99.9 | 99.9 | 99.9 | 99.9 | 40.2 | 40.2 | 13.1 | 39.9 | 99.9 |
| Exit Gas Equivalence Ratio | 0.269 | 0.418 | 0.022 | 0.024 | 0.012 | 0.012 | 0.069 | 0.046 | 0.220 | 0.032 | 0.034 |
| % Excess Air | 272 | 139 | 4524 | 4052 | 8325 | 7958 | 1348 | 2070 | 355 | 3041 | 2826 |
| PDTF Pressure (psig) | 5.2 | 25.6 | 126 | 132 | 130 | 128 | 99 | 92 | 11.6 | 23.0 | 35.7 |
| Zone 1 Tube Temp. (°C) | 1164 | 1259 | 1263 | 1282 | 1097 | 1382 | 1468 | 1497 | 1098 | 1098 | 1098 |
| Zone 2 Tube Temp. (°C) | 1253 | 1298 | 1280 | 1297 | 1098 | 1406 | 1463 | 1499 | 1098 | 1097 | 1098 |
| Zone 3 Tube Temp. (°C) | 1296 | 1295 | 955 | 964 | 840 | 1082 | 1127 | 1209 | 1096 | 1096 | 1092 |
| Optical Zone Temp. (°C) | 1035 | 1053 | 880 | 893 | 724 | 1029 | 892 | 905 | 871 | 909 | 906 |
| Zone 4 Tube Temp. (°C) | 1262 | 1296 | 921 | 916 | 866 | 951 | 898 | 973 | 1098 | 1097 | 1097 |
| Substrate Metal Temp. (°C) | 176 | 343 | 250 | 211 | 157 | 223 | 98 | 106 | 37 | 142 | 176 |
| Prim. Gas Vel. (m/s) | 7.62 | 3.73 | 2.12 | 2.04 | 2.07 | 2.13 | 2.66 | 2.84 | 4.63 | 4.07 | 3.02 |
| Total Gas Vel. (m/s) | 1.15 | 1.42 | 0.35 | 0.34 | 0.31 | 0.38 | 0.18 | 0.20 | 0.25 | 0.53 | 0.99 |
| Accelerator Gas Vel. (m/s) | 41.5 | 51.1 | 12.6 | 12.2 | 11.1 | 13.8 | 6.5 | 7.3 | 9.0 | 19.2 | 35.6 |
| Avg. Residence Time (s) | 0.35 | 0.28 | 1.1 | 1.2 | 1.3 | 1.0 | 2.2 | 2.0 | 1.6 | 0.75 | 0.40 |

TABLE 12

Operating Conditions and Results from Fly Ash Combustion Tests Using Allison Fuel Spring Creek Coal

| | AFSPC26 | AFSPC27 | AFSPC28 | AFSPC33 | AFSPC34 | AFSPC35 | APSPC44 | APSPC45 | APSPC46 |
|--------------------------------------|---------|---------|---------|---------|---------|---------|---------|---------|---------|
| Coal Feed Rate (g/min) | 0.5264 | 0.4016 | 0.4728 | 0.5350 | 0.3490 | 0.3794 | 0.3195 | 0.3173 | 0.3483 |
| Total Weight Coal Fed (g) | 10.3 | 8.3 | 16.2 | 20.4 | 14.7 | 11.8 | 17.3 | 16.4 | 18.0 |
| Weight Ash Collected (g) | 0.3037 | 0.1706 | 0.5063 | 0.468 | 3.1863 | 3.1104 | 0.3336 | 2.8343 | 4.0964 |
| Weight Ash Feed (g) | 0.454 | 0.367 | 0.715 | 0.901 | 0.649 | 0.521 | 0.764 | 0.724 | 0.795 |
| Percent Ash in Fly Ash (mf) | ND | 77.8 | 70.5 | 79.9 | 12.2 | 10.1 | 44.5 | 8.35 | 8.64 |
| Fly Ash Carbon Burnout (%) | ND | 98.6 | 98.0 | 98.8 | 65.1 | 57.0 | 94.0 | 47.1 | 49.0 |
| Avg. Feeder Air Flow Rate (slpm) | 8.0 | 10.0 | 10.0 | 10.0 | 10.0 | 10.0 | 20.0 | 20.0 | 20.0 |
| Avg. Sec. Air Flow Rate (slpm) | 5.0 | 30.1 | 30.0 | 30.0 | 30.2 | 30.2 | 20.1 | 20.1 | 20.1 |
| Avg. N ₂ Flow Rate (slpm) | 13.1 | 40.1 | 40.3 | 40.0 | 40.2 | 40.1 | 40.3 | 40.3 | 40.3 |
| Exit Gas Equivalence Ratio | 0.280 | 0.070 | 0.082 | 0.093 | 0.060 | 0.065 | 0.055 | 0.055 | 0.060 |
| % Excess Air | 257 | 1338 | 1121 | 979 | 1560 | 1427 | 1710 | 1723 | 1560 |
| PDTF Pressure (psig) | 4.3 | 11.2 | 3.2 | 3.9 | 102.9 | 105.8 | 107.8 | 109.6 | 107.8 |
| Zone 1 Tube Temp. (°C) | 1497 | 1484 | 1298 | 1482 | 1474 | 1298 | 1298 | 1493 | 1419 |
| Zone 2 Tube Temp. (°C) | 1498 | 1496 | 1298 | 1498 | 1498 | 1298 | 1298 | 1485 | 1343 |
| Zone 3 Tube Temp. (°C) | 1495 | 1495 | 1295 | 1496 | 1216 | 1057 | 1035 | 1156 | 895 |
| Optical Zone Temp. (°C) | 1182 | 1186 | 1049 | 1139 | 979 | 866 | 921 | 937 | 762 |
| Zone 4 Tube Temp. (°C) | 1320 | 1326 | 1274 | 1281 | 922 | 881 | 929 | 918 | 802 |
| Substrate Metal Temp. (°C) | 65 | 111 | 128 | 135 | 140 | 123 | 103 | 111 | 100 |
| Prim. Gas Vel. (m/s) | 6.38 | 5.86 | 8.43 | 8.24 | 1.30 | 1.27 | 2.49 | 2.46 | 2.50 |
| Total Gas Vel. (m/s) | 0.45 | 1.00 | 1.29 | 1.40 | 0.19 | 0.16 | 0.16 | 0.17 | 0.14 |
| Accelerator Gas Vel. (m/s) | 16.0 | 36.1 | 46.3 | 50.3 | 6.7 | 5.8 | 5.6 | 6.1 | 5.0 |
| Avg. Residence Time (s) | 0.90 | 0.40 | 0.31 | 0.29 | 2.15 | 2.47 | 2.55 | 2.37 | 2.86 |

TABLE 13

Operating Conditions from Fly Ash Combustion Tests Using
PC/AC/HWD/Micronized Spring Creek Coal

| | APSPC29 | APSPC32 | APSPC39 | APSPC40 |
|--------------------------------------|---------|---------|---------|---------|
| Coal Feed Rate (g/min) | 0.3742 | 0.1440 | 0.1330 | 0.2267 |
| Total Weight Coal Fed (g) | 18.1 | 13.5 | 13.4 | 11.6 |
| Weight Ash Collected (g) | 1.0076 | 0.5667 | 0.5122 | 0.2424 |
| Weight Ash Feed (g) | 0.799 | 0.596 | 0.592 | 0.512 |
| Percent Ash in Fly Ash (mf) | 13.8 | 20.0 | 46.5 | 58.6 |
| Fly Ash Carbon Burnout (%) | 86.7 | 91.5 | 97.6 | 98.5 |
| Avg. Feeder Air Flow Rate (slpm) | 10.0 | 9.8 | 20.0 | 20.0 |
| Avg. Sec. Air Flow Rate (slpm) | 30.0 | 30.0 | 20.2 | 20.2 |
| Avg. N ₂ Flow Rate (slpm) | 40.0 | 40.3 | 40.3 | 40.3 |
| Exit Gas Equivalence Ratio | 0.065 | 0.025 | 0.023 | 0.039 |
| % Excess Air | 1442 | 3886 | 4258 | 2456 |
| PDTF Pressure (psig) | 3.4 | 3.5 | 105.0 | 107.2 |
| Zone 1 Tube Temp. (°C) | 1298 | 1485 | 1298 | 1492 |
| Zone 2 Tube Temp. (°C) | 1298 | 1498 | 1298 | 1487 |
| Zone 3 Tube Temp. (°C) | 1295 | 1496 | 1027 | 1170 |
| Optical Zone Temp. (°C) | 1055 | 1167 | 850 | 903 |
| Zone 4 Tube Temp. (°C) | 1276 | 1307 | 856 | 862 |
| Substrate Metal Temp. (°C) | 125 | 140 | 111 | 124 |
| Prim. Gas Vel. (m/s) | 8.36 | 8.21 | 2.55 | 2.50 |
| Total Gas Vel. (m/s) | 1.27 | 1.42 | 0.16 | 0.17 |
| Accelerator Gas Vel. (m/s) | 45.6 | 51.3 | 5.8 | 6.3 |
| Avg. Residence Time (s) | 0.32 | 0.28 | 2.50 | 2.30 |

5.0 CONCLUSIONS AND FUTURE PLANS

1. Detailed chemical and mineralogic analysis for the raw and hydrothermally treated coal revealed that most of the salts of organic acid groups and soluble minerals are removed by the beneficiation process.
2. The CCSEM results indicated that although the processing into CWF reduced the total amounts of inorganic constituents present, the relative amounts of discrete minerals remained constant. That is, no significant reduction occurred in any one mineral category over another.

3. The size analysis of the CCSEM data indicates that the CWF coal was dominated by minerals in the 2.2- to 4.6-micrometer size range, while the size distribution of minerals in the raw coal was much more dispersed.
4. The changes in particle size and amounts of organically associated inorganics brought about by the beneficiation process may be important factors when considering ash behavior because they affect both the ash particle chemistry and aerodynamic behavior in the utilization system.
5. The addition of kaolin reduced the amount of sodium species present in the small size fractions ($< 1 \mu\text{m}$) by a factor of two. This indicates that the kaolin was acting as an alkali getter for the vapor-phase sodium species.
6. Beneficiation of the Spring Creek fuel by physical/acid cleaning, hot-water drying, and micronizing and just hot-water drying and micronizing both decreased the concentration of sodium species in the small size fractions. This decrease is due to the removal of significant quantities of sodium cations in the beneficiation process.
7. There is some evidence to indicate that deep cleaning the fuel might actually increase the concentration of sodium species in the small size fractions by removing inorganic species which act as effective alkali getters. Further investigation of this premise is required before solid conclusions can be made.

Further PETF testing with other beneficiated Spring Creek fuels is planned to determine the effect of the individual cleaning steps on the removal of selected inorganic species.

6.0 REFERENCES

1. Swanson, M.L.; Mann, M.D.; Moe, T.A. "Turbine Combustion Phenomena," Annual Report Contract No. DE-FC21-86MC10637, 1989, p 71.
2. Maas, D.J. et al. "Advanced Processes for Premium Low-Rank Coal/Water Fuel Production," Annual Technical Report for the Period April 1, 1987, to March 31, 1988, Prepared for the U.S. Department of Energy (DE-FC21-86MC-10637), 1988.
3. Chari, M.V. Bechtel National, "Thermal Upgrading of Low-Rank Coals, A Process Survey," Fifth Annual EPRI Contractors Conference on Coal Gasification, Palo Alto, CA, October 30-31, 1985.
4. Swanson, M.L.; Mann, M.D.; Hajicek, D.R.; Maas, D.J. "Combustion of Low-Rank Coal/Water Slurries Under Gas Turbine Operating Conditions", *In* Proceedings of the 13th International Conference on Coal and Slurry Technology; Denver, CO, April 12-15, 1988, pp 391-398.
5. Swanson, M.L.; Mann M.D. "Turbine Combustion Phenomena," Annual Technical Report for the Period April 1, 1987 - March 31, 1988.
6. Swanson, M.L.; Mann, M.D.; Potas, T.A. "Comparison of Coal/Water Fuels Performance in a Gas Turbine Combustor," Fourteenth Inter. Conf. on Coal & Slurry Technology, April 24-27, 1989, pp 353-364.

TABLE 14

Operating Conditions and Results from Fly Ash Combustion Tests
Using Raw Spring Creek Coal and Spring Creek Coal Mixed with
Kaolin for Alkali Gettering

| | SPCRK30 | SPCRK31 | SPCRK37 | SPCRK38 | SPRCK41 | SPRCK42 w/Kaol. | SPCRK43 w/Kaol. |
|--------------------------------------|---------|---------|---------|---------|---------|--------------------|--------------------|
| Coal Feed Rate (g/min) | 1.1835 | 1.0299 | 0.7932 | 0.9048 | 1.0122 | 0.5169 | 0.5677 |
| Total Weight Coal Fed (g) | 27.3 | 21.8 | 19.5 | 26.3 | 20.8 | 18.4 | 26.2 |
| Weight Ash Collected (g) | 1.6491 | 1.1468 | 0.3106 | 0.3387 | 0.8145 | 0.6004 | 0.1972 |
| Weight Ash Feed (g) | 1.341 | 1.070 | 0.958 | 1.291 | 1.021 | 1.290 | 1.836 |
| Percent Ash in Fly Ash (mf) | 35.2 | 37.2 | 86.8 | 90.4 | 37.0 | 69.5 | 89.2 |
| Fly Ash Carbon Burnout (%) | 90.1 | 90.9 | 99.2 | 99.4 | 90.8 | 96.8 | 99.1 |
| Avg. Feeder Air Flow Rate (slpm) | 10.0 | 10.0 | 20.0 | 19.3 | 5.0 | 5.0 | 20.0 |
| Avg. Sec. Air Flow Rate (slpm) | 30.0 | 30.0 | 20.1 | 20.2 | 0.0 | 0.0 | 20.1 |
| Avg. N ₂ Flow Rate (slpm) | 40.0 | 40.2 | 40.1 | 40.3 | 5.1 | 5.1 | 40.0 |
| Exit Gas Equivalence Ratio | 0.197 | 0.171 | 0.132 | 0.152 | 1.374 | 0.685 | 0.092 |
| % Excess Air | 408 | 484 | 660 | 556 | 0 | 46 | 987 |
| PDTF Pressure (psig) | 4.9 | 5.5 | 109.3 | 107.6 | 1.9 | 1.9 | 109.2 |
| Zone 1 Tube Temp. (°C) | 1298 | 1484 | 1498 | 1298 | 1497 | 1497 | 1498 |
| Zone 2 Tube Temp. (°C) | 1298 | 1498 | 1494 | 1298 | 1498 | 1498 | 1498 |
| Zone 3 Tube Temp. (°C) | 1295 | 1496 | 1176 | 1034 | 1495 | 1496 | 1211 |
| Optical Zone Temp. (°C) | 1039 | 1192 | 921 | 831 | 1041 | 1061 | 1053 |
| Zone 4 Tube Temp. (°C) | 1267 | 1321 | 903 | 938 | 1097 | 1098 | 981 |
| Substrate Metal Temp. (°C) | 123 | 132 | 122 | 96 | 31 | 30 | 121 |
| Prim. Gas Vel. (m/s) | 7.79 | 7.55 | 2.47 | 2.40 | 4.61 | 4.61 | 2.48 |
| Total Gas Vel. (m/s) | 1.18 | 1.29 | 0.17 | 0.16 | 0.19 | 0.19 | 0.18 |
| Accelerator Gas Vel. (m/s) | 42.4 | 46.5 | 6.2 | 5.6 | 7.0 | 7.0 | 6.3 |
| Avg. Residence Time (s) | 0.34 | 0.31 | 2.34 | 2.57 | 2.06 | 2.05 | 2.28 |

7. Jones, M.L.; Kalmanovitch, D.P.; Steadman, E.N.; Benson, S.A.
"Application of SEM Techniques to the Characterization of Coal and Coal
Ash Products," H.L.C. Meuzelaar, Ed., *Advances in Coal Spectroscopy*,
1992, p 1-27.
8. Kalmanovitch, D.P.; Montgomery, G.G.; Steadman, E.N. ASME Paper Number
87-JPGC-FACT-4, 1987.
9. Steadman, E.N.; Benson, S.A.; Zygarlicke, C.J.; Brekke, D.W.
"Characterization of Liquid Phase Components in Coal Ashes and Deposits,"
*In Proceedings of the Seventh Annual International Pittsburgh Coal
Conference; September 14-18, 1990.*

TABLE 15

SEMP and XRD Analyses--Multicyclone Fly Ash Samples

| Run #: | SPCRK037 | SPCRK037 | SPCRK037 | | | |
|---|--------------|------------------|--------------|------------------|-------------|------------------|
| Collection Device: | Cyclone #2 | Cyclone #5 | Final Filter | | | |
| Fuel Type: | Spring Creek | Spring Creek | Spring Creek | | | |
| Sample Weights (g) | 0.2558 | 0.0225 | 0.0323 | | | |
| Particle Size by Malvern 2600 | | | | | | |
| Sample Mean Size (μm) | 15.4 | 19.5 | 60.3 | | | |
| Sample Top Size (99% \lt , μm) | 72.2 | 119.8 | 420.0 | | | |
| Total Number of Points | 293 | 249 | 249 | | | |
| Particle Types, % of Total Counts | | | | | | |
| Crystalline Phases | | | | | | |
| Akermanite | 0.7 | 0.0 | 0.0 | | | |
| Gehlenite | 2.0 | 1.6 | 0.0 | | | |
| Anorthite | 1.4 | 0.0 | 0.0 | | | |
| Albite | 1.0 | 0.0 | 0.0 | | | |
| Nepheline | 0.3 | 0.0 | 0.0 | | | |
| Pyroxene | 0.3 | 0.0 | 0.0 | | | |
| Spurrite | 0.0 | 0.4 | 0.0 | | | |
| Calcium Aluminate | 4.4 | 1.2 | 0.0 | | | |
| Quartz | 33.8 | 0.4 | 0.0 | | | |
| Iron Oxide | 0.7 | 0.0 | 0.0 | | | |
| Ankerite (Ca, Mg, Fe)CO ₃ | 0.3 | 0.0 | 0.0 | | | |
| Aluminum Oxide | 0.3 | 0.0 | 0.0 | | | |
| Dolomite | 1.4 | 0.0 | 0.0 | | | |
| Barite | 0.3 | 0.4 | 0.0 | | | |
| Sodium Sulfate | 0.0 | 0.0 | 7.6 | | | |
| Unclassified and Amorphous Phases | | | | | | |
| Unclassified | 32.8 | 95.6 | 92.4 | | | |
| Pure Kaolinite (Amorp.) | 13.0 | 0.0 | 0.0 | | | |
| Kaolinite-Derived | 4.1 | 0.4 | 0.0 | | | |
| Illite (Amorp.) | 0.7 | 0.0 | 0.0 | | | |
| Montmorillonite (Amorp.) | 2.0 | 0.0 | 0.0 | | | |
| Calcium-Derived | 0.3 | 0.0 | 0.0 | | | |
| Average Composition (wt%) | <u>Bulk</u> | <u>Amorphous</u> | <u>Bulk</u> | <u>Amorphous</u> | <u>Bulk</u> | <u>Amorphous</u> |
| SiO ₂ | 56.8 | 42.1 | 12.5 | 12.6 | 1.0 | 5.6 |
| Al ₂ O ₃ | 17.6 | 27.5 | 22.6 | 23.6 | 0.6 | 2.9 |
| Fe ₂ O ₃ | 3.9 | 4.7 | 11.8 | 12.3 | 2.9 | 4.1 |
| TiO ₂ | 1.1 | 1.6 | 2.1 | 2.1 | 0.1 | 0.0 |
| P ₂ O ₅ | 0.1 | 0.1 | 0.4 | 0.4 | 0.2 | 0.6 |
| CaO | 12.7 | 15.3 | 34.9 | 36.2 | 3.5 | 5.0 |
| MgO | 3.5 | 3.8 | 8.9 | 9.4 | 2.0 | 3.3 |
| Na ₂ O | 3.2 | 4.5 | 3.1 | 3.3 | 43.5 | 73.1 |
| K ₂ O | 0.3 | 0.4 | 0.1 | 0.1 | 2.9 | 5.4 |
| SO ₃ | 0.7 | 0.0 | 3.5 | 0.0 | 43.4 | 0.0 |
| X-Ray Diffraction Results | | | | | | |
| Quartz, SiO ₂ | Major | | NA | | | ND |
| Mullite, Al ₂ Si ₂ O ₇ | Minor | | NA | | | ND |
| Cristobalite, SiO ₂ | Minor | | NA | | | ND |
| Lime, CaO | Minor | | NA | | | ND |
| Periclase, MgO | Minor | | NA | | | ND |
| Sodium Sulfate, Na ₂ SO ₄ | ND | | NA | | | Major |
| Iron Silicide, Fe ₂ Si | ND | | NA | | | Major |

TABLE 16

SEMPC and XRD Analyses--Multicyclone Fly Ash Samples Run APSPC040

| Run #: | APSPC040 | | APSPC040 | | APSPC040 | |
|--|---------------|------------------|---------------|------------------|---------------|------------------|
| Collection Device: | Cyclone #2 | | Cyclone #5 | | Final Filter | |
| Cleaning: | Acid/Physical | | Acid/Physical | | Acid/Physical | |
| Fuel Type: | Spring Creek | | Spring Creek | | Spring Creek | |
| Sample Weights (g) | 0.1934 | | 0.0235 | | 0.0255 | |
| Particle Size by Malvern 2600 | | | | | | |
| Sample Mean Size (μm) | 15.1 | | 10.4 | | 30.7 | |
| Sample Top Size (99%<, μm) | 77.5 | | 46.3 | | 130.5 | |
| Total Number of Points | 248 | | 248 | | 102 | |
| Particle Types, % of Total Counts | | | | | | |
| Crystalline Phases | | | | | | |
| Gehlenite | 2.0 | | 0.0 | | 0.0 | |
| Anorthite | 6.5 | | 0.8 | | 0.0 | |
| Albite | 3.6 | | 0.8 | | 0.0 | |
| Nepheline | 0.4 | | 0.8 | | 0.0 | |
| Pyroxene | 0.4 | | 0.4 | | 0.0 | |
| Mullite | 0.4 | | 0.0 | | 0.0 | |
| Spurrite | 0.4 | | 0.0 | | 0.0 | |
| Häüyne | 0.4 | | 0.8 | | 0.0 | |
| Spinel | 0.4 | | 0.0 | | 0.0 | |
| Quartz | 13.3 | | 2.0 | | 0.0 | |
| Iron Oxide | 1.2 | | 0.0 | | 0.0 | |
| Calcium Oxide | 0.8 | | 0.0 | | 0.0 | |
| Sodium Sulfate | 0.4 | | 0.0 | | 1.0 | |
| Sodium Calcium Sulfate | 0.4 | | 0.4 | | 0.0 | |
| Unclassified and Amorphous Phases | | | | | | |
| Unclassified | 48.0 | | 90.3 | | 99.0 | |
| Pure Kaolinite (Amorp.) | 10.5 | | 0.0 | | 0.0 | |
| Kaolinite-Derived | 5.6 | | 3.2 | | 0.0 | |
| Montmorillonite (Amorp.) | 5.2 | | 0.4 | | 0.0 | |
| Average Composition (wt%) | <u>Bulk</u> | <u>Amorphous</u> | <u>Bulk</u> | <u>Amorphous</u> | <u>Bulk</u> | <u>Amorphous</u> |
| SiO ₂ | 45.2 | 41.3 | 24.2 | 23.6 | 5.3 | 8.8 |
| Al ₂ O ₃ | 25.4 | 31.8 | 32.5 | 35.9 | 6.5 | 11.5 |
| Fe ₂ O ₃ | 5.1 | 5.2 | 14.4 | 14.8 | 15.2 | 21.4 |
| TiO ₂ | 1.3 | 1.3 | 2.0 | 2.3 | 0.3 | 0.6 |
| P ₂ O ₅ | 0.1 | 0.1 | 0.4 | 0.5 | 1.9 | 2.6 |
| CaO | 9.6 | 10.2 | 9.2 | 10.1 | 1.9 | 3.2 |
| MgO | 3.2 | 4.0 | 4.4 | 4.8 | 6.5 | 9.2 |
| Na ₂ O | 5.0 | 5.6 | 7.2 | 7.6 | 39.3 | 40.6 |
| K ₂ O | 0.3 | 0.4 | 0.2 | 0.4 | 1.3 | 2.0 |
| SO ₃ | 4.8 | 0.0 | 5.4 | 0.0 | 21.8 | 0.0 |
| X-Ray Diffraction Results | Not Available | | | | | |

10. Steadman, E.N.; Erickson T.A. "Coal and Ash Characterization--Digital Image Analysis Applications," Engineering Foundation Conference, Inorganic Transformations and Ash Deposition During Combustion, Palm Coast, FL, March 10-15, 1991.
11. Benson, S.A.; Holm, P.L. "Comparison of the Inorganic Constituents in Low-Rank Coals," *Ind. Eng. Chem. Prod. Res. Dev.* 1985, 24, 145.

TABLE 17

SEMP and XRD Analyses--Multicyclone Fly Ash Samples Run SPCRK041

| Run #: | SPCRK041 | | SPCRK041 | | SPCRK041 | |
|---|--------------|------------------|--------------|------------------|--------------|------------------|
| Collection Device: | Cyclone #2 | | Cyclone #5 | | Final Filter | |
| Fuel Type: | Spring Creek | | Spring Creek | | Spring Creek | |
| Sample Weights (g) | 0.7201 | | 0.0584 | | 0.0360 | |
| Particle Size by Malvern 2600 | | | | | | |
| Sample Mean Size (μm) | 30.4 | | 9.6 | | 54.6 | |
| Sample Top Size (99%<, μm) | 509.0 | | 77.5 | | 161.1 | |
| Total Number of Points | 85 | | 249 | | 252 | |
| Particle Types, % of Total Counts | | | | | | |
| Crystalline Phases | | | | | | |
| Gehlenite | 1.2 | | 4.0 | | 0.0 | |
| Anorthite | 4.7 | | 1.2 | | 0.0 | |
| Calcium Aluminate | 3.5 | | 2.0 | | 0.0 | |
| Quartz | 27.1 | | 0.0 | | 0.0 | |
| Iron Oxide | 0.0 | | 0.4 | | 0.0 | |
| Calcium Oxide | 2.4 | | 2.4 | | 0.0 | |
| Ankerite (Ca, Mg, Fe)CO ₃ | 1.2 | | 0.4 | | 0.0 | |
| Dolomite | 0.0 | | 0.4 | | 0.0 | |
| Barite | 1.2 | | 0.0 | | 0.0 | |
| Sodium Sulfate | 0.0 | | 0.0 | | 5.2 | |
| Sodium Calcium Sulfate | 1.2 | | 0.4 | | 1.6 | |
| Unclassified and Amorphous Phases | | | | | | |
| Unclassified | 42.4 | | 88.4 | | 93.3 | |
| Pure Kaolinite (Amorp.) | 5.9 | | 0.0 | | 0.0 | |
| Kaolinite-Derived | 8.2 | | 0.4 | | 0.0 | |
| Montmorillonite (Amorp.) | 1.2 | | 0.0 | | 0.0 | |
| Average Composition (wt%) | <u>Bulk</u> | <u>Amorphous</u> | <u>Bulk</u> | <u>Amorphous</u> | <u>Bulk</u> | <u>Amorphous</u> |
| SiO ₂ | 49.7 | 37.8 | 20.7 | 22.2 | 2.4 | 6.1 |
| Al ₂ O ₃ | 19.7 | 27.5 | 23.1 | 24.0 | 1.9 | 4.6 |
| Fe ₂ O ₃ | 4.5 | 5.7 | 8.9 | 9.2 | 2.1 | 4.8 |
| TiO ₂ | 1.3 | 2.1 | 1.3 | 1.3 | 0.2 | 0.4 |
| P ₂ O ₅ | 0.1 | 0.1 | 0.2 | 0.2 | 0.2 | 0.6 |
| CaO | 16.2 | 17.1 | 32.3 | 31.5 | 5.2 | 11.7 |
| MgO | 3.8 | 5.2 | 8.2 | 8.2 | 1.1 | 2.4 |
| Na ₂ O | 3.2 | 4.1 | 3.2 | 3.3 | 31.9 | 66.4 |
| K ₂ O | 0.2 | 0.3 | 0.1 | 0.1 | 1.6 | 2.9 |
| SO ₃ | 1.3 | 0.0 | 2.1 | 0.0 | 53.3 | 0.0 |
| X-Ray Diffraction Results | | | | | | |
| Quartz, SiO ₂ | Minor | | Minor | | Minor | |
| Lime, CaO | ND | | Minor | | ND | |
| Periclase, MgO | ND | | Minor | | ND | |
| Sodium Sulfate, Na ₂ SO ₄ | ND | | ND | | Minor | |
| Bredigite, Ca ₂ Mg ₂ (SiO ₄) ₂ | ND | | ND | | Minor | |

TABLE 18

SEMP and XRD Analyses--Multicyclone Fly Ash Samples Run SPCRK042

| Run #: | SPCRK042 | | SPCRK042 | | SPCRK042 | |
|--|------------------------|------------------|------------------------|------------------|------------------------|------------------|
| Collection Device: | Cyclone #2 | | Cyclone #5 | | Final Filter | |
| Fuel Type: | Spring Creek w/ Kaolin | | Spring Creek w/ Kaolin | | Spring Creek w/ Kaolin | |
| Sample Weights (g) | 0.4716 | | 0.1125 | | 0.0163 | |
| Particle Size by Malvern 2600 | | | | | | |
| Sample Mean Size (μm) | 32.8 | | 20.9 | | 83.2 | |
| Sample Top Size (99%<, μm) | 461.8 | | 108.3 | | 370.3 | |
| Total Number of Points | 249 | | 249 | | 249 | |
| Particle Types, % of Total Counts | | | | | | |
| Crystalline Phases | | | | | | |
| Gehlenite | 12.4 | | 9.6 | | 0.0 | |
| Anorthite | 5.2 | | 22.5 | | 0.0 | |
| Albite | 0.4 | | 0.0 | | 0.0 | |
| Nepheline | 0.0 | | 0.0 | | 0.4 | |
| Mullite | 0.0 | | 0.4 | | 0.0 | |
| Häuyne | 0.4 | | 0.0 | | 0.4 | |
| Calcium Aluminate | 1.6 | | 0.0 | | 0.0 | |
| Quartz | 9.2 | | 0.0 | | 0.0 | |
| Iron Oxide | 0.4 | | 0.0 | | 0.0 | |
| Calcium Oxide | 1.2 | | 0.4 | | 0.0 | |
| Aluminum Oxide | 0.4 | | 0.0 | | 0.0 | |
| Rutile | 0.4 | | 0.0 | | 0.0 | |
| Dolomite | 0.4 | | 0.0 | | 0.0 | |
| Barite | 0.3 | | 0.0 | | 0.0 | |
| Anhydrite | 1.2 | | 0.0 | | 0.0 | |
| Sodium Calcium Sulfate | 0.8 | | 0.0 | | 0.4 | |
| Ferric Sulfate | 0.4 | | 0.0 | | 0.0 | |
| Unclassified and Amorphous Phases | | | | | | |
| Unclassified | 31.3 | | 55.8 | | 98.8 | |
| Pure Kaolinite (Amorp.) | 18.1 | | 0.0 | | 0.0 | |
| Kaolinite-Derived | 12.9 | | 10.8 | | 0.0 | |
| Illite (Amorp.) | 0.4 | | 0.0 | | 0.0 | |
| Montmorillonite (Amorp.) | 2.4 | | 0.4 | | 0.0 | |
| | | | | | 0.0 | |
| Average Composition (wt%) | <u>Bulk</u> | <u>Amorphous</u> | <u>Bulk</u> | <u>Amorphous</u> | <u>Bulk</u> | <u>Amorphous</u> |
| SiO ₂ | 42.2 | 42.2 | 34.6 | 33.5 | 11.6 | 18.6 |
| Al ₂ O ₃ | 27.9 | 32.9 | 32.8 | 32.4 | 9.9 | 15.9 |
| Fe ₂ O ₃ | 3.7 | 3.2 | 4.3 | 4.7 | 2.7 | 4.5 |
| TiO ₂ | 1.6 | 1.4 | 1.7 | 1.9 | 1.0 | 1.6 |
| P ₂ O ₅ | 0.3 | 0.5 | 0.2 | 0.4 | 0.7 | 1.1 |
| CaO | 14.5 | 12.1 | 15.8 | 17.0 | 5.9 | 9.6 |
| MgO | 3.3 | 3.0 | 4.0 | 4.4 | 1.7 | 2.8 |
| Na ₂ O | 3.8 | 4.4 | 5.7 | 5.5 | 25.7 | 42.5 |
| K ₂ O | 0.3 | 0.3 | 0.2 | 0.2 | 2.1 | 3.4 |
| SO ₃ | 2.5 | 0.0 | 0.6 | 0.0 | 38.7 | 0.0 |
| X-Ray Diffraction Results | | | | | | |
| Quartz, SiO ₂ | Minor | | Major | | Minor | |
| Anhydrite, CaSO ₄ | ND | | ND | | Minor | |
| Pyrrhotite, Fe _{1-x} S | ND | | ND | | Minor | |

TABLE 19

SEMPC and XRD Analyses--Multicyclone Fly Ash Samples Run SPCRK043

| Run #: | SPCRK043 | SPCRK043 | SPCRK043 |
|---|------------------------|------------------------|------------------------|
| Collection Device: | Cyclone #2 | Cyclone #5 | Final Filter |
| Fuel Type: | Spring Creek w/ Kaolin | Spring Creek w/ Kaolin | Spring Creek w/ Kaolin |
| Sample Weights (g) | 0.1572 | 0.0322 | 0.0078 |
| Particle Size by Malvern 2600 | | | |
| Sample Mean Size (μm) | 15.5 | 8.6 | 36.4 |
| Sample Top Size (99%<, μm) | 64.4 | 101.4 | 148.0 |
| Total Number of Points | 249 | 249 | 249 |
| Particle Types, % of Total Counts | | | |
| Crystalline Phases | | | |
| Gehlenite | 10.8 | 5.6 | 0.0 |
| Anorthite | 4.8 | 7.2 | 0.0 |
| Albite | 0.4 | 0.0 | 0.0 |
| Nepheline | 0.8 | 0.4 | 0.0 |
| Häuyne | 0.4 | 0.4 | 0.0 |
| Quartz | 8.0 | 0.0 | 0.0 |
| Iron Oxide | 0.4 | 0.0 | 0.0 |
| Calcium Oxide | 0.4 | 0.0 | 0.0 |
| Barite | 1.2 | 0.0 | 0.0 |
| Sodium Sulfate | 0.0 | 0.0 | 8.8 |
| Unclassified and Amorphous Phases | | | |
| Unclassified | 43.8 | 83.5 | 91.2 |
| Pure Kaolinite (Amorp.) | 19.3 | 0.0 | 0.0 |
| Kaolinite-Derived | 8.0 | 2.8 | 0.0 |
| Montmorillonite (Amorp.) | 1.6 | 0.0 | 0.0 |
| Average Composition (wt%) | | | |
| | <u>Bulk</u> | <u>Amorphous</u> | <u>Bulk</u> |
| | | | <u>Amorphous</u> |
| | <u>Bulk</u> | <u>Amorphous</u> | <u>Bulk</u> |
| | | | <u>Amorphous</u> |
| SiO ₂ | 41.8 | 39.1 | 28.5 |
| Al ₂ O ₃ | 29.7 | 33.2 | 30.5 |
| Fe ₂ O ₃ | 3.7 | 3.6 | 6.3 |
| TiO ₂ | 1.2 | 1.4 | 2.1 |
| P ₂ O ₅ | 0.1 | 0.1 | 0.5 |
| CaO | 14.1 | 14.1 | 19.2 |
| MgO | 3.2 | 3.1 | 5.4 |
| Na ₂ O | 4.7 | 5.1 | 6.2 |
| K ₂ O | 0.3 | 0.3 | 0.1 |
| SO ₃ | 1.3 | 0.0 | 1.2 |
| X-Ray Diffraction Results | | | |
| Quartz, SiO ₂ | Minor | Minor | ND |
| Mullite, Al ₂ Si ₂ O ₇ | Minor | ND | ND |
| Periclase, MgO | Minor | Minor | ND |
| Pyrrhotite-6C, Fe _{1-x} S | Minor | ND | ND |
| Iron Silicide, Fe ₂ Si | ND | ND | Minor |
| Sodium Sulfate, Na ₂ SO ₄ | ND | ND | Major |
| Ferrite Spinel, (Mg, Fe)(Fe, Al) ₂ O ₄ | ND | Minor | ND |

TABLE 20

SEMP and XRD Analyses--Multicyclone Fly Ash Samples Run AFSPC045

| Pin #: | AFSPC045 | AFSPC045 | AFSPC045 | | | |
|--|------------------------------|------------------------------|------------------------------|------------------|-------------|------------------|
| Collection Device: | Cyclone #2 | Cyclone #5 | Final Filter | | | |
| Fuel Type: | Allison Fuel Spring Creek | Allison Fuel Spring Creek | Allison Fuel Spring Creek | | | |
| Sample Weights (g) | 2.1765 | 0.0768 | 0.5810 | | | |
| Particle Size by Malvern 2600 | | | | | | |
| Sample Mean Size (μm) | 19.9 | 18.6 | 10.6 | | | |
| Sample Top Size (99%<, μm) | 131.9 | 48.1 | 68.2 | | | |
| Total Number of Points | 51 | 40 | 169 | | | |
| Particle Types, % of Total Counts | | | | | | |
| Crystalline Phases | | | | | | |
| Gehlenite | 9.8 | 7.5 | 0.6 | | | |
| Anorthite | 0.0 | 0.0 | 1.8 | | | |
| Albite | 0.0 | 2.5 | 0.0 | | | |
| Calcium Aluminate | 0.0 | 2.5 | 0.0 | | | |
| Quartz | 17.6 | 40.0 | 0.6 | | | |
| Iron Oxide | 2.0 | 2.5 | 0.0 | | | |
| Pyrite | 2.0 | 0.0 | 0.0 | | | |
| Unclassified and Amorphous Phases | | | | | | |
| Unclassified | 52.9 | 25.0 | 92.3 | | | |
| Pure Kaolinite (Amorp.) | 5.9 | 17.5 | 2.4 | | | |
| Kaolinite-Derived | 5.9 | 0.0 | 2.4 | | | |
| Illite (Amorp) | 2.0 | 0.0 | 0.0 | | | |
| Montmorillonite (Amorp.) | 2.0 | 2.5 | 0.0 | | | |
| Average Composition (wt%) | <u>Bulk</u> | <u>Amorphous</u> | <u>Bulk</u> | <u>Amorphous</u> | <u>Bulk</u> | <u>Amorphous</u> |
| SiO ₂ | 38.6 | 29.9 | 70.0 | 46.3 | 9.1 | 27.7 |
| Al ₂ O ₃ | 20.9 | 27.7 | 15.1 | 33.1 | 7.8 | 27.1 |
| Fe ₂ O ₃ | 4.8 | 3.6 | 0.5 | 0.0 | 4.0 | 4.4 |
| TiO ₂ | 1.3 | 1.9 | 0.4 | 0.9 | 0.2 | 0.5 |
| P ₂ O ₅ | 0.1 | 0.1 | 0.1 | 0.2 | 0.8 | 0.5 |
| CaO | 17.1 | 20.8 | 8.3 | 14.5 | 6.6 | 14.6 |
| MgO | 5.7 | 7.1 | 1.8 | 2.8 | 8.7 | 7.6 |
| Na ₂ O | 5.8 | 8.4 | 1.8 | 2.2 | 37.3 | 17.1 |
| K ₂ O | 0.4 | 0.5 | 0.0 | 0.0 | 1.2 | 0.5 |
| SO ₃ | 5.2 | 0.0 | 2.1 | 0.0 | 24.3 | 0.0 |
| X-Ray Diffraction Results | Not Available | | | | | |

12. Nowok, J.W.; Benson, S.A.; Jones, M.L.; Kalmanovitch, D.P. "Sintering Behavior and Strength Development in Various Coal Ashes," *Fuel* 1990, 69, 1020-1029.

13. Wenglarz, A.; Ames, F.; Fox, R.; Wilkes C.; Williams, J. "Gas Turbine Screening Program," final report for DOE Contract DOE/MC/21394-2199 (DE87001057), December 1986, 85 p.

U.S. DEPARTMENT OF ENERGY
FEDERAL ASSISTANCE MANAGEMENT SUMMARY REPORT

| | | |
|--|---|--|
| 1. Program/Project Identification No DE-FC21-86MC10637 | 2. Program/Project Title Turbine Combustion Phenomena (3.1) | 3. Reporting Period 4-1-92 through 8-30-92 |
| 4. Name and Address Energy and Environmental Research Center University of North Dakota Box 8213, University Station, Grand Forks, ND 58202 (701) 777-5000 | | 5. Program/Project Start Date 4-1-86 |
| | | 6. Completion Date 9-30-92 |

| 7. FY 91/92 | 8. Months or Quarters Quarters | 1991 | | | | | | 1992 | | | | | | | | | | | |
|---|-----------------------------------|-----------------------------------|-----|-----|-----|--------------|-----------|------|-----|-----|-----|-----|-----|-----|--|--|--|--|--|
| | | JUL | AUG | SEP | OCT | NOV | DEC | JAN | FEB | MAR | APR | MAY | JUN | | | | | | |
| 9. Cost Status | | a. Dollars Expressed in Thousands | | | | | | | | | | | | | | | | | |
| | | b. Dollar Scale | | | | | | | | | | | | | | | | | |
| 10. Cost Chart | | | | | | | | | | | | | | | | | | | |
| Fund Source | | Quarter | | | | Cum. to Date | Tot. Plan | | | | | | | | | | | | |
| | | 1st | 2nd | 3rd | 4th | | | | | | | | | | | | | | |
| DOE | P | 63 | 63 | 63 | 62 | 251 | 251 | | | | | | | | | | | | |
| | A | 54 | 30 | 37 | 64 | 185 | | | | | | | | | | | | | |
| | P | | | | | | | | | | | | | | | | | | |
| | A | | | | | | | | | | | | | | | | | | |
| | P | | | | | | | | | | | | | | | | | | |
| | A | | | | | | | | | | | | | | | | | | |
| | P | | | | | | | | | | | | | | | | | | |
| | A | | | | | | | | | | | | | | | | | | |
| Total P | | 63 | 63 | 63 | 62 | 251 | 251 | | | | | | | | | | | | |
| Total A | | 54 | 30 | 37 | 64 | 185 | | | | | | | | | | | | | |
| Variance | | 9 | 33 | 26 | (2) | 66 | | | | | | | | | | | | | |
| | | P = Planned A = Actual | | | | | | | | | | | | | | | | | |
| Total Planned Costs for Program/Project | | c. Cumulative Accrued Costs | | | | | | | | | | | | | | | | | |
| | | Planned | | 63 | | | 126 | | | | 189 | | | 251 | | | | | |
| | | Actual | | 54 | | | 84 | | | | 121 | | | 185 | | | | | |
| | | Variance | | 9 | | | 42 | | | | 68 | | | 66 | | | | | |
| | | \$251 | | | | | | | | | | | | | | | | | |

| 11. Major Milestone Status | Units Planned | | Description |
|--|---------------|---|--|
| | P | C | |
| A. Revised Technology and Market Assessment | | | No activities in current project year. |
| B. Characterization of LRCs' Atomization Properties | | | No activities in current project year. |
| C. Evaluation of LRC Fuel Agglomeration | | | No activities in current project year. |
| D. Investigation of Particulate Hot-Gas Cleanup Systems | | | 1 ▽ 2 Δ |
| E-1. Ash Transformation Studies for Beneficiated LRC Fuels | | | 1 ▽ 2 Δ |
| E-2. PETF Additive Testing for Improved Ash Characteristics | | | Δ |
| F. Investigation of Slagging Combustor Design | | | No activities in current project year. |
| G. Baseline Combustion Test with Spring Creek Fuel Utilized in GM Allison Combustion Tests | | | |
| H. Final Report | | | |

12. Remarks
Due to EERC fiscal year end, the June books do not close until July 25, 1992. Costs posted through July 8 have been included.

13. Signature of Recipient and Date
Michael J. Johnson 7-29-92

14. Signature of DOE Reviewing Representative and Date

U.S. DEPARTMENT OF ENERGY
FEDERAL ASSISTANCE MANAGEMENT SUMMARY REPORT

| 1. Program/Project Identification No. DE-FC21-86MC10637 | | 2. Program/Project Title Turbine Combustion Phenomena (3.1) | | 3. Reporting Period 4-1-92 through 6-30-92 | |
|---|--|--|------------------------|---|--|
| 4. Name and Address Energy and Environmental Research Center University of North Dakota Box 8213, University Station Grand Forks, ND 58202 (701) 777-5000 | | | | 5. Program/Project Start Date 4-1-86 | |
| | | | | 6. Completion Date 9-30-92 | |
| Milestone ID. No. | Description | Planned Completion Date | Actual Completion Date | Comments | |
| Task A | Revised Technology and Market Assessment -- Completed in Year 4 -- | | | | |
| Task B | Characterization of LRCs' Atomization Properties -- Completed in Year 5 -- | | | | |
| Task C | Evaluation of LRC Fuel Agglomeration -- No activities in Year 6 -- | | | | |
| Task D d.1 | Investigation of Particulate Hot-Gas Cleanup Systems: Design and construct ceramic barrier filter probes for conducting long-term testing in the pressurized drop-tube furnace (PDTF) | 1-31-92 | | | |
| d.2 | Conduct two long-term ceramic barrier filter tests to examine filter performance and ceramic material degradation. | 6-15-92 | | | |
| Task E E-1.1 | Ash Transformation Studies: Perform ash transformation studies for beneficiated LRC fuels. | 1-31-92 | | Moved back due to other project use of PDTF | |
| E-2.1 | Construct slurry droplet feed system for PDTF. | 10-31-91 | | | |
| E-2.2 | Perform additive testing for improved ash characteristics. | 1-31-92 | | Moved back due to other project use of PDTF | |
| Task F | Investigation of Slagging Combustor Design -- No work planned for Year 6 -- | | | | |
| Task G | Baseline Combustion Test with Spring Creek Fuel Utilized in GM Allison Combustion Tests | 2-29-92 | | | |
| Task H | Final Report | 8-31-92 | | | |